NASA CR-165157
PWA-5594-122

NASA-CR-165157
19810006487

NASA

ENERGY EFFICIENT ENGINE
DIFFUSER/COMBUSTOR MODEL TECHNOLOGY REPORT

Prepared
by

W.B. Gardner, Program Manager
Energy Efficient Engine Component
Development and Integration Program

UNITED TECHNOLOGIES CORPORATION
Pratt & Whitney Aircraft Group
Commercial Products Division

Prepared for
NATIONAL AERONAUTICS AND SPACE ADMINISTRATION
NASA-Lewis Research Center
Contract NAS3-20646

CR 165157

"Energy Efficient Engine Deffuser/Combuster Model Technology Report Draft"

By W. B. Gardner

United Tech. P W Nas 3-20646

CR 165158 (former No. CR 165157)

"Measurement of Rod Seal Lubrication for Stirling Engine Application"

By Allen I.Kranter

Shaker Research Inc. DEN 3-22

1 Report No	2 Government Accession No	3 Recipient's Catalog No
NASA CR-165157		

4 Title and Subtitle	5 Report Date
Energy Efficient Engine Diffuser/Combustor Model Technology Report	June 1980
	6 Performing Organization Code

7 Author(s)	8 Performing Organization Report No
W.B. Gardner, et al	PWA-5594-122
	10 Work Unit No

9 Performing Organization Name and Address	11 Contract or Grant No
UNITED TECHNOLOGIES CORPORATION Pratt & Whitney Aircraft Group Commercial Products Division	NAS3-20646
	13 Type of Report and Period Covered

12 Sponsoring Agency Name and Address	14 Sponsoring Agency Code
National Aeronautics and Space Administration Lewis Research Center 21000 Brookpark Road, Cleveland, Ohio 44135	Technology Report

15 Supplementary Notes

Project Manager: N.T. Saunders, NASA Lewis Research Center, Cleveland, Ohio 44135

16 Abstract

A full-scale, full-annular diffuser/combustor model test rig was tested to investigate how configurational changes affect pressure loss and flow separation characteristics. The rig was characterized by five major modules: inlet, prediffuser, strut, simulated combustor, and full combustor. The prediffuser featured a short, curved-wall, dump design. Performance goals included (1) a separation-free prediffuser flow field, (2) total pressure loss limited to 3.0 percent in the prediffuser and shrouds, and (3) an overall section pressure loss of 5.5 percent P_{T3} at the design airflow distribution. Test results indicated that the prediffuser configurations operated well within the program goals for pressure loss and demonstrated separation-free operation over a wide range of inlet conditions.

17 Key Words (Suggested by Author(s))		18 Distribution Statement
Diffuser/Combustor	Shroud	Unclassified - Unlimited
Modular Rig	Dump Gap	
Separation-Free	Flow Split	
Prediffuser	Profile	

19 Security Classif (of this report)	20 Security Classif (of this page)	21 No of Pages	22 Price*
Unclassified	Unclassified		

* For sale by the National Technical Information Service Springfield Virginia 22161

N81-15002 #

This Page Intentionally Left Blank

FOREWORD

The Energy Efficient Engine Component Development and Integration Program is being conducted under parallel National Aeronautics and Space Administration contracts with Pratt & Whitney Aircraft Group and General Electric Company. The overall project is under the direction of Mr. Neal T. Saunders. Mr. John W. Schaefer is the NASA assistant project manager for the Pratt & Whitney Aircraft effort under NASA contract NAS3-20646, and Mr. Daniel E. Sokolowski is the NASA project engineer responsible for the portion of the project described in this report. Mr. William B. Gardner is manager of the Energy Efficient Engine program at Pratt & Whitney Aircraft Group, and Dr. W.B. Wagner, Dr. S. Tanrikut, and Mr. R. McKinney are the engineers responsible for the work described in this report.

This Page Intentionally Left Blank

TABLE OF CONTENTS

LIST OF ILLUSTRATIONS

LIST OF ILLUSTRATIONS (Continued)

LIST OF ILLUSTRATIONS (Continued)

LIST OF ABBREVIATIONS AND SYMBOLS

A	-	cross sectional area
α	-	profile energy coefficient, $\frac{1}{A}\int_o^A \left(\frac{u}{\bar{U}}\right)^3 dA$
AR	-	prediffuser exit to inlet area ratio
B	-	blockage factor, $1 - \frac{1}{A}\int_o^A \frac{u}{U_{max}} dA$
β	-	prediffuser flow turning angle
R	-	Radius from engine centerline
Δ R	-	prediffuser inlet annulus height
η	-	prediffuser efficiency: C_{p1-2}/C_p ideal
L	-	prediffuser axial length
Mn	-	Mach Number
P_s	-	static pressure
P_t	-	total pressure
q	-	dynamic pressure
Re	-	Reynolds number based on hydraulic diameter
u	-	axial velocity
W_A	-	mass flow rate (measured)
X	-	dump gap spacing
Cp_{1-x}	-	static pressure recovery coefficient to axial station x, $(\tilde{P}_{sx} - \tilde{P}_{s_1})/\bar{q}_1$
Cp_{ideal}	-	one-dimensional, incompressible flow; $1 - AR^2$
λ_{1-3}	-	total pressure loss to axial station x, $(\bar{P}_{t1} - \bar{P}_{tx})/\bar{P}_{t1}$

Subscripts

1,2,3	-	axial stations
i or ID	-	inner annulus or inner diameter
o or OD	-	outer annulus or outer diameter
max	-	maximum value

Superscripts

$\bar{(\ )}$	-	mass averaged quantity
$\tilde{(\ )}$	-	arithmetic average

1.0 SUMMARY

The purpose of the Energy Efficient Engine diffuser/combustor model program was to experimentally document and optimize the aerodynamic performance of the prediffuser/combustor section. To accomplish this, a full-scale, full-annular modular rig was designed and tested to investigate the effects of various configurational changes on pressure loss and flow separation characteristics. The established performance goals included (1) a separation-free prediffuser flow field, (2) total pressure loss limited to 3.0 percent in the prediffuser and shrouds, and (3) an overall section pressure loss of 5.5 percent P_{T3} at the design airflow distribution.

Program results indicated that the prediffuser configurations operated well within the program goals for pressure loss and demonstrated separation-free operation over a wide range of inlet conditions. The dump gap between the prediffuser and combustor hood influenced system performance more than any of the other design parameters tested. Changes in flow split, combustor radial location, inlet profile, and bleed air extraction exhibited minimal effects on system performance. Almost all of the pressure rise of a given system occurred in the prediffuser, while almost all of the pressure loss occurred in the dump, hood, and annuli regions.

2.0 INTRODUCTION

The objective of the NASA Energy Efficient Engine Component Development and Integration Program is to develop, evaluate, and demonstrate the technology for achieving lower installed specific fuel consumption and lower operating costs in future commercial turbofan engines. NASA has set minimum goals of 12 percent reduction in thrust specific fuel consumption (TSFC), 5 percent reduction in direct operating costs (DOC), and 50 percent reduction in performance degradation for the Energy Efficient Engine (flight propulsion system) relative to the JT9D-7A reference engine. In addition, environmental goals on emissions (meet the proposed EPA 1981 regulation) and noise (meet FAR 36-1978 standards) were established at the beginning of the program.

The following performance goals were established for the diffuser/combustor model test program: (1) demonstrate a separation-free prediffuser flow field, (2) limit the total pressure loss in the prediffuser and shrouds to 3.0 percent P_{T3}, and (3) demonstrate an overall section pressure loss of 5.5 percent P_{T3} at the design airflow distribution. Resultant data from these efforts were used to recommend a design of the diffuser/combustor model for use in the combustor sector rig and combustor component efforts. The diffuser/combustor model test program was conducted to ensure timely interaction with the component effort as shown in Figure 1.

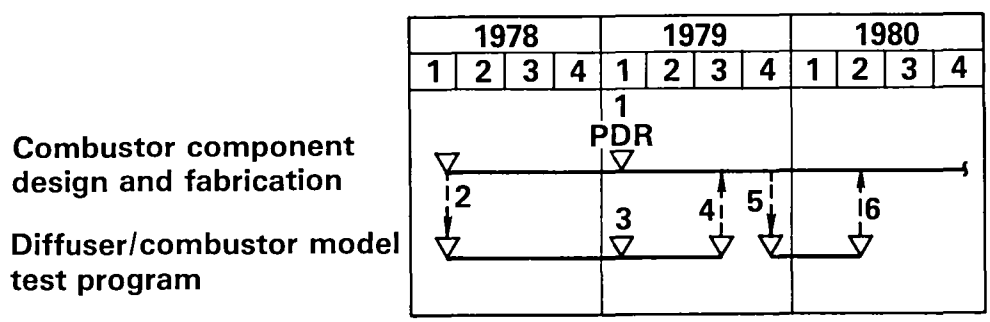

1 — Component Preliminary Design Review (PDR) completed, detailed design initiated
2 — Component flowpath and aerodynamic characteristics specified
3 — Baseline design verified
4 — Evaluation of alternate designs completed, diffuser/combustor aerodynamics specified
5 — Modified strut geometry specified
6 — Modified strut aerodynamic impact determined

Figure 1 Interaction of Energy Efficient Engine Combustor Programs - The diffuser/combustor model test program was conducted to ensure timely interaction with the component effort.

To substantiate design predictions (see section 3.1), a full-scale, full-annular Plexiglas model of the prediffuser/combustor section was designed and fabricated. The model consisted of an inlet module, a prediffuser module, strut module, simulated combustor module, and the full combustor module. The modular design feature made it easier to investigate how pressure loss and flow separation margin were affected by changes in prediffuser case contour, combustor hood geometry, and inlet conditions.

This report presents the program procedures and results obtained from evaluating the various test models used in the program. The test procedure, including a description of the rig modules, is presented in section 3.3. Section 4.0 presents the program test results.

3.0 PROGRAM PROCEDURES

3.1 Analysis and Design

The analysis and design effort was conducted to provide fabrication drawings and specifications necessary to ensure the proper modeling of the prediffuser/combustor flowpaths and aerodynamic characteristics (Figure 2) specified in the combustor component preliminary design. A modular design approach was employed to expedite the assembly and configuration turnaround during the test program. The rig design consisted of five major modules: inlet, prediffuser, strut, simulated combustor, and full combustor. A detailed description of the various modules is presented in section 3.3.3. A schematic of the full-scale, full-annular airflow rig developed for this program is shown in Figure 3.

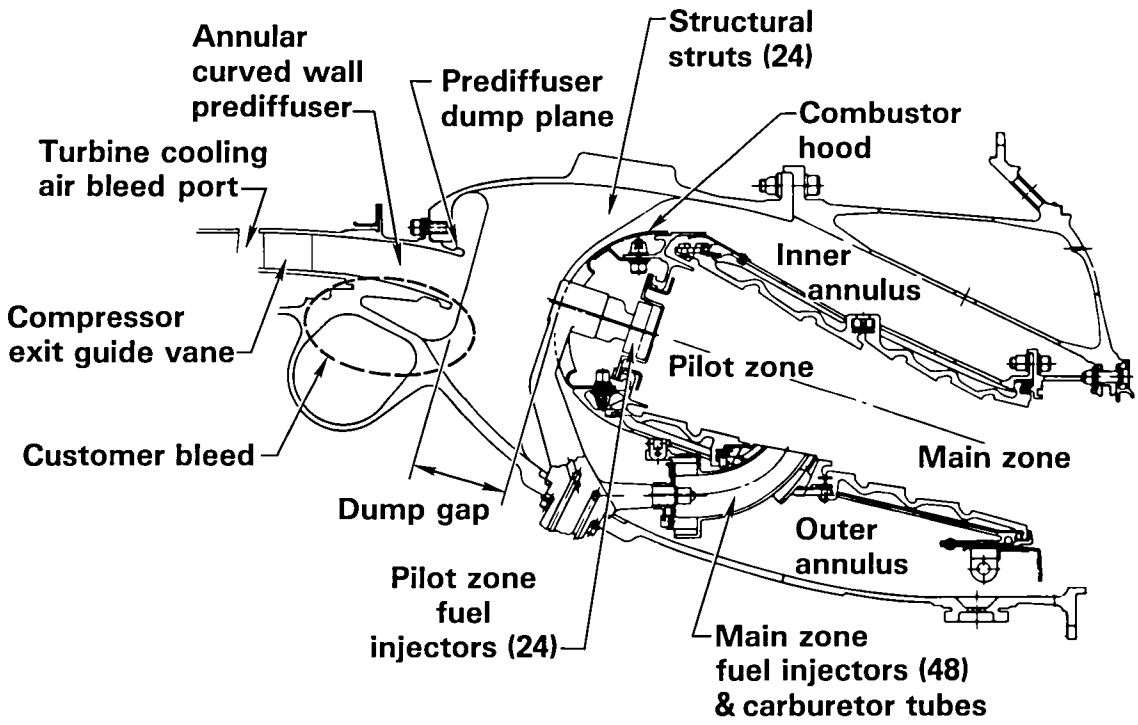

Figure 2 Energy Efficient Engine Combustor Cross-Section

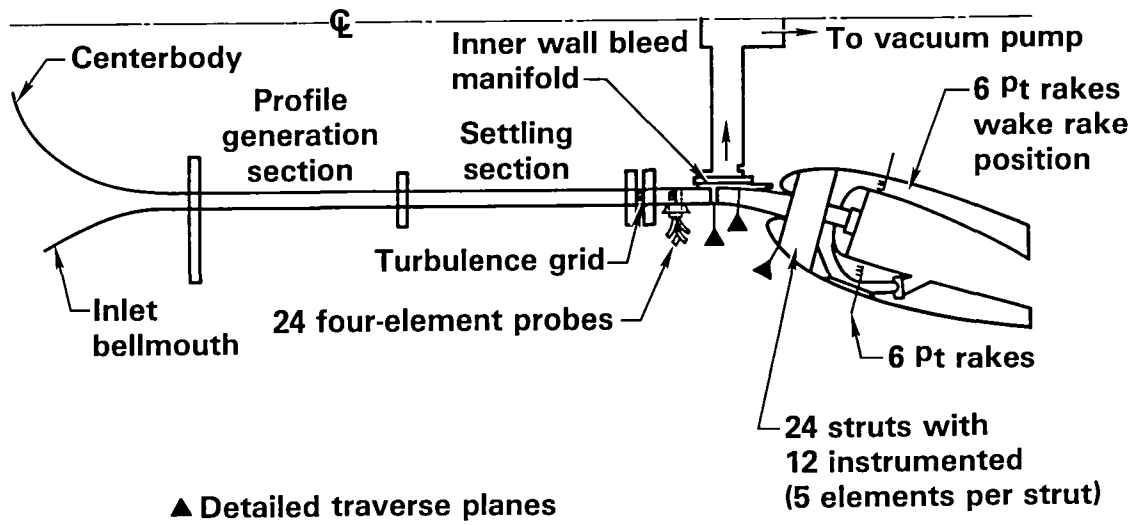

Figure 3 Test Rig Assembly

The rig design incorporated a high degree of flexibility. This provided for rapid changes in rig configuration, thereby reducing the amount of time between tests and ensuring efficient operation of the program. Transparent Plexiglas in the flowpath permitted flow visualization techniques to be employed throughout the test program.

The analysis and design effort identified several curved wall prediffuser geometries as well as the associated downstream hardware to be evaluated in the test program. The two-dimensional, axisymmetric, analytical model used in the component preliminary design was employed to provide configurations in addition to the baseline engine design. The analytical model allowed variations in inlet profile conditions and accommodated curved wall contours. Prediffuser length, amount of turning, and rate of diffusion were varied to identify configurations that operated separation-free. The geometric characteristics of the three configurations selected for testing are specified in Table 1 and Figure 4. Configuration I was the baseline design. Configuration II, by virtue of the increased area ratio and reduced exit Mach number, offered a potential reduction in the prediffuser dump losses. Possibility of reduced section weight was investigated with the shorter prediffuser (Configuration III).

TABLE 1

GEOMETRIC CHARACTERISTICS OF CONFIGURATIONS TESTED

Configuration	Ri/Ro	L/ΔR	Area Ratio	β*
I (Baseline)	0.92	3.5	1.50	14°
II	0.92	3.5	1.57	10°
III	0.92	3.0	1.50	14°

* Includes 5-degree wall cant prior to prediffuser inlet.

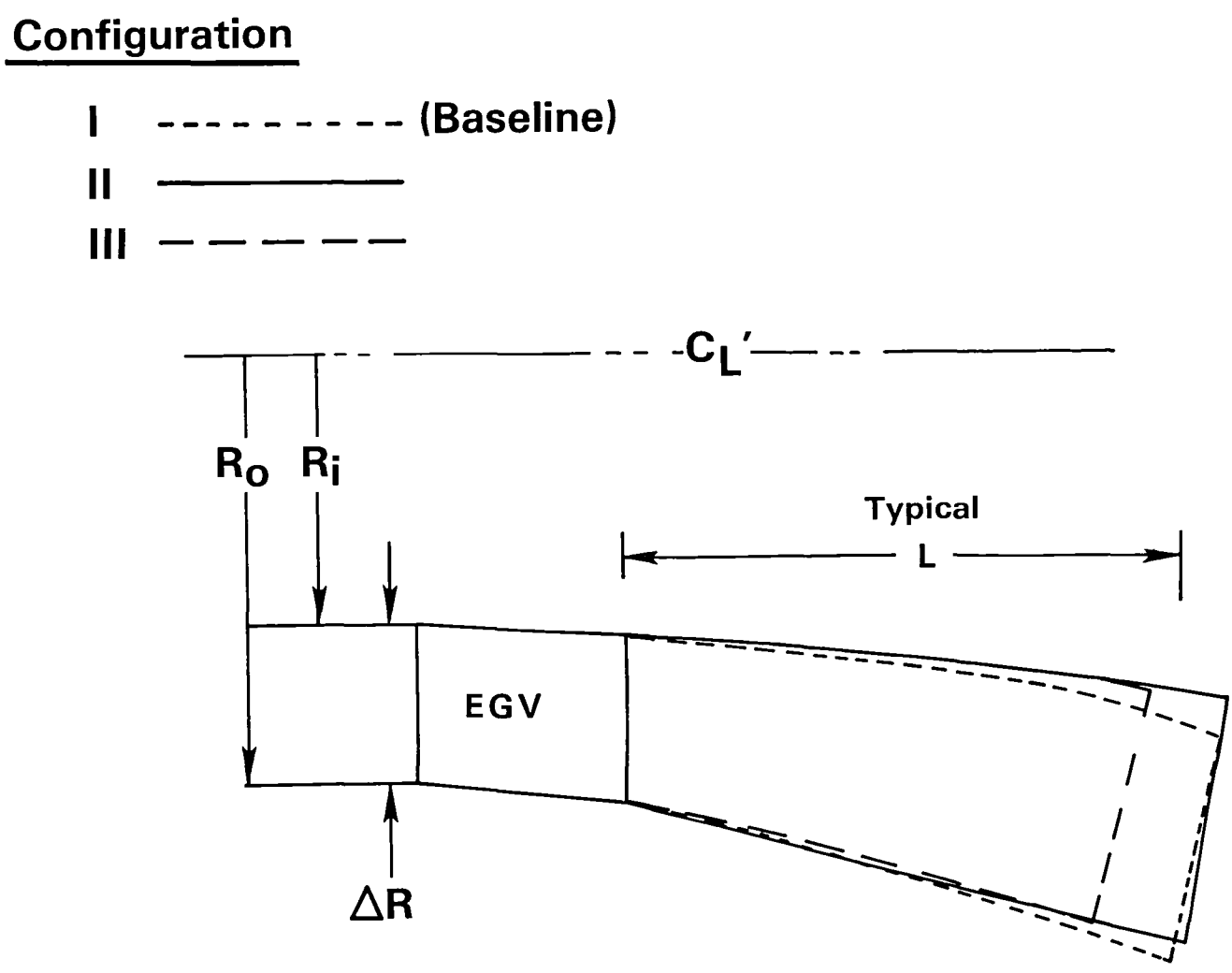

Figure 4 Comparison of the Three Prediffuser Contours Tested

The predicted pressure recovery coefficient of the baseline configuration I corresponded to an average diffuser efficiency (Cp/Cp_{ideal}) of approximately 75 percent. Positive values of the skin friction coefficient for the outer wall, deemed the critical area, indicated separation-free operation of the prediffuser. The pressure rise and skin friction coefficients are presented in Figure 5. Similar results were obtained for configurations II and III.

The design of total pressure probes and static pressure instrumentation required to completely specify the combustor section flow field was established. A computer program to process and reduce the data was also developed.

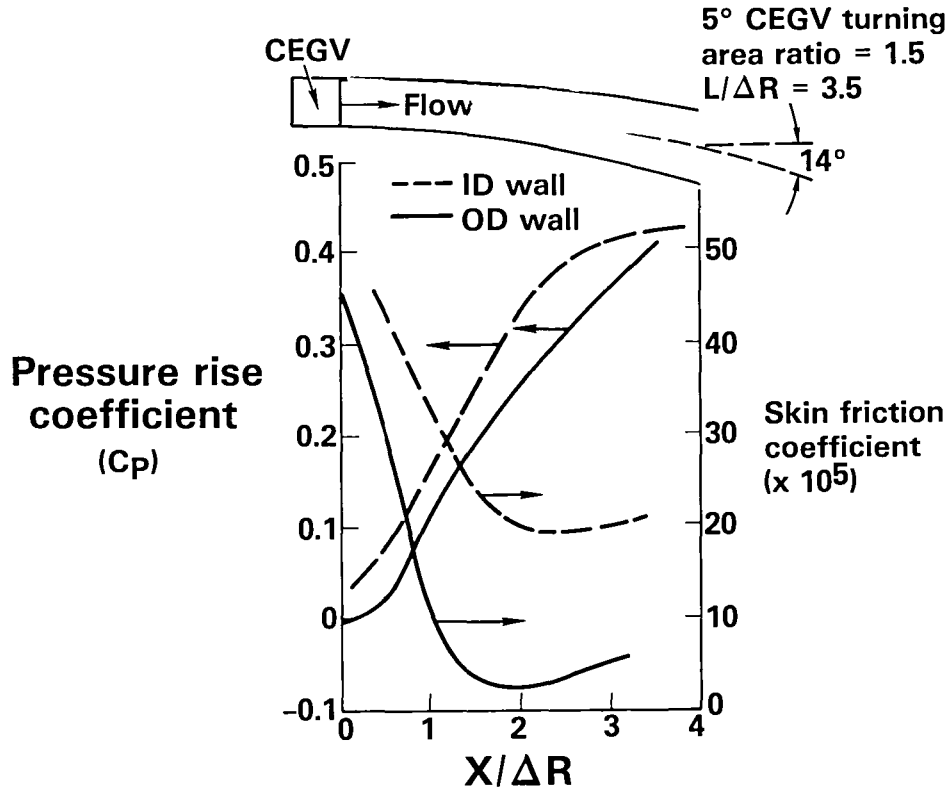

Figure 5 Baseline (Configuration I) Prediffuser Performance Prediction

3.2 Fabrication and Assembl

The test rig met all design requirements. Design features employing wood and Plexiglas were incorporated so that the reduced weight facilitated rig handling at the test stand. The test rig properly modeled combustor flowpaths and achieved the high degree of flexibility needed to fully investigate the system aerodynamic performance. The fabrication and assembly of the test configurations provided the hardware required for each phase of the testing sequence. The prediffuser module hardware was fabricated for the initial prediffuser inlet flow characterization tests. The strut section, simulated combustor, and full combustor modules were fabricated during the prediffuser performance tests. Information gained from each phase of the test program was used to facilitate subsequent assembly. Rig hardware was initially instrumented during the fabrication stage, but the rig design made it easy to install additional instrumentation at the test facility.

3.3 Test

3.3.1 General Description

Several prediffusers were tested both with and without modeled combustor hardware installed downstream. This determined the best possible aerodynamic configuration of components within the combustor section. Data were processed and analyzed after each test sequence to assess combustor section aerodynamic performance and to formulate model modifications required to improve the design. Several prediffuser contours were evaluated to determine pressure recovery and flow separation margins. Prediffuser inlet total pressure profile was varied to determine the sensitivity of a particular wall contour to inlet profile. The effect of dump region geometry on airflow distribution and pressure loss was investigated. Hood capture areas and hood openings around pilot fuel injector supports were varied in order to minimize total pressure losses.

Combustor section flowpaths and configurations that met the program aerodynamic goals were identified in the diffuser/combustor model test program. The optimum design features were incorporated in the sector rig and component programs.

3.3.2 Test Facility

Testing was conducted in an airflow test facility used for development testing of diffusers and for basic studies of mixing and diffusion. Air was delivered to the rig at flow rates up to 4.5 kg/s (10 pps) at 28 kpa (4 psig) pressure. Inlet temperature ranged between 294 and 333 K (70 and 140 F). Inlet ducting was equipped with a 59.9-cm (24-in.) control valve and a flat-plate orifice for airflow measurement. The rig was mounted directly on the inlet duct and discharged to ambient air in the test cell. A 0.24 M^3/s (500 scfm) vacuum pump extracted auxiliary bleed flows. The entire test operation was monitored from an adjacent control room in which the necessary equipment was located to properly set and measure test conditions and control the data acquisition system.

3.3.3 Rig Description and Instrumention

The parametric nature of the experimental program required a versatile test rig that permitted efficient configurational changes. To meet this requirement and to expedite assembly and disassembly, the rig consisted of five major modules: (1) inlet, (2) prediffuser, (3) strut, (4) simulated combustor, and (5) full combustor. Each of these modules is discussed in sections 3.3.3.1 through 3.3.3.5. The rig instrumentation is listed in Table 2.

TABLE 2
DIFFUSER RIG INSTRUMENTATION LIST

Location	Measurement/Type	Quantity	Purpose
Inlet Module	4 element total pressure (PT) probes	24	Prediffuser inlet PT profiles
	ID/OD wall static pressure (PS) taps	24/24	
Prediffuser Module	ID wall PS taps (12 rows) OD wall PS taps (12 rows)	7/row 7/row	Prediffuser performance
Strut Module	5 leading edge PT's	12 struts	Prediffuser exit profile
Simulated Combustor Module			
Outer Shroud	Kielhead PT's	3	
Inner Shroud	Kielhead PT's	3	Verification of flow splits
Hood	Kielhead PT's	3	
Inner Shroud	11 element wake rake	2 positions	Diffuser case strut wake characteristics
Full Combustor Module			
Outer Shroud	8 rows wall PS 4 element PT rakes	4 each row 6	
Inner Shroud	6 rows wall PS 3 element PT rakes	4 each row 6	Combustor pressure field
Outer Liner	8 rows wall PS	4 each row	
Inner Liner	6 rows wall PS	3 each row	
Hood	Kielhead PT's	3	

3.3.3.1 Inlet Module

The rig inlet module comprised an inlet bellmouth/centerbody assembly (to provide the transition from circular to annular flow), a series of straight annular ducts, and a swirl generation section. An assembly of the various inlet sections is shown in Figure 6. The first of the annular ducts had provisions to install layers of screens on either the inner or outer wall to generate a radial total pressure profile. A settling section, following the profile generation section, reduced the non-equilibrium disturbances produced in the profile generation section. Each section of the rig inlet module comprised at the upstream and downstream end six axial support struts (0.16 cm (0.062 in.) thick and 2.54 cm (1.0 in.) long) to maintain the proper annulus spacing.

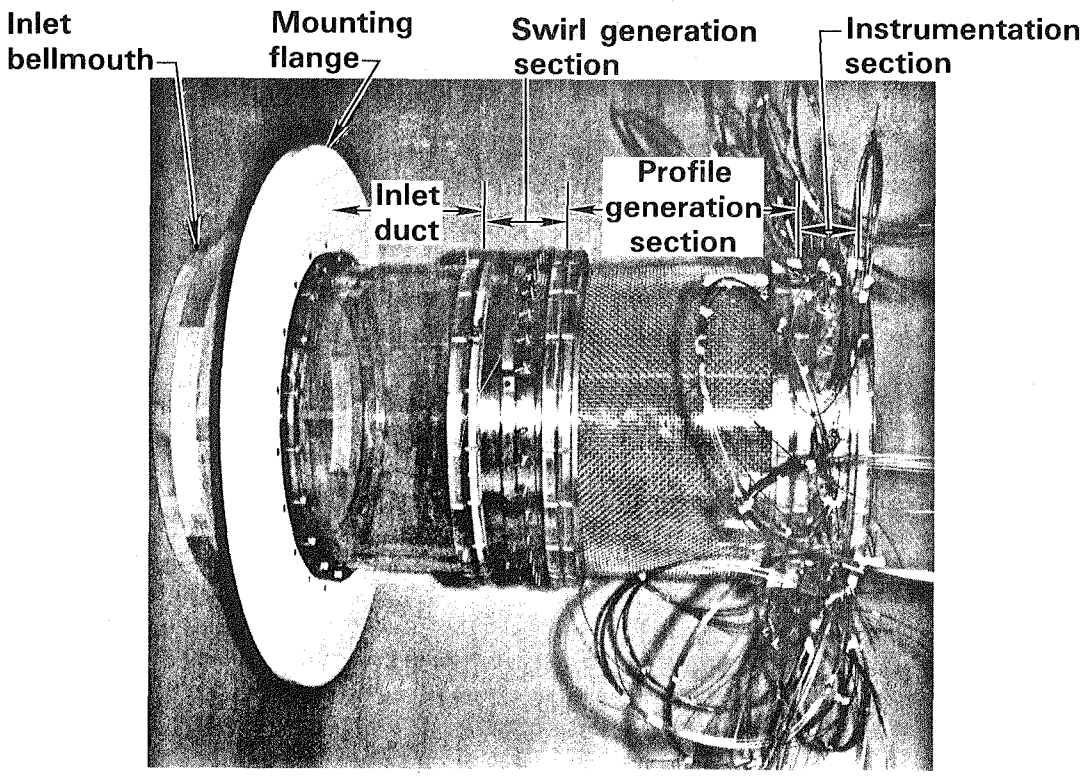

Figure 6 Diffuser/Combustor Model Rig Inlet Module Hardware Assembly

The purpose of the swirl generation section was to simulate the swirling flow from the last rotor of the compressor. This section consisted of a steel duct which included 36 individual vanes. These vanes were linked to a unison ring such that the rotation of the ring resulted in an equal movement of each swirl vane. The maximum turning angle in the swirl vanes was approximately 60 degrees. A wire grid normal to the flow could be inserted upstream of the instrumentation section to vary the core flow turbulence intensity level.

The instrumentation section had provisions for 24 four-element total pressure probes (Figure 7) and included an equal number of static pressure taps on the inner and outer walls. All probes were used in the inlet flow characterization tests to ascertain the degree of circumferential uniformity in the flow field approaching the prediffuser module inlet. In the subsequent performance evaluation tests, the number of probes was reduced to six to minimize downstream propagation of wakes from the probes.

Figure 7 Installation of Inlet Total Pressure Probes

3.3.3.2 Prediffuser Module

Three interchangeable prediffuser modules followed the instrumentation section. The principal variables addressed by these configurations were length, area ratio, and turning angle. The prediffuser module included a compressor exit guide vane assembly upstream of each prediffuser configuration. The compressor exit guide vane assembly consisted of a 29 mm (1.15 in.) annulus with an outward 5-degree cant on each wall. Seventy-four curved exit guide vanes were included in the annulus. This assembly ensured an axial inlet flow for all prediffuser performance tests using the swirl generation section. An additional section was fabricated with the same 5-degree cant, but the 74 exit vanes were replaced with 6 thin axial support struts to ensure proper spacing between the inner and outer walls. This second assembly permitted prediffuser testing without swirling of the inlet flow. A 0.65 mm (0.25 in.) wide full-annular slot on the inner wall at the leading edge of the canted duct provided a method for simulating the turbine cooling air bleed. Modulated air extraction was accomplished using a 0.24 M^3/s (500 scfm) vacuum pump.

Each prediffuser wall contained a longitudinal row of seven equally spaced static pressure taps at twelve circumferential locations. Ten of the rows were located circumferentially between the downstream diffuser case struts and the remaining two were directly in-line with a strut.

3.3.3.3 Strut Module

The strut section (see Figure 8) formed the dump region downstream of the prediffuser. The 24 diffuser case struts acted as structural members and initially were shaped aerodynamically to minimize the propagation of wakes into the inner and outer shroud annuli. Twelve of the diffuser case struts had five leading edge total pressure probes (Figure 9) to measure the prediffuser exit profile.

3.3.3.4 Simulated Combustor Module

Either a full combustor module or a simulated combustor module could be installed downstream of the strut module. Each prediffuser configuration had its own hood/bulkhead assembly with the center of the hood positioned radially near mid-span of the prediffuser exit annulus. Thus simulated combustor modules were used in the early phase of the investigation because of the relative ease of fabrication compared to a full combustor module.

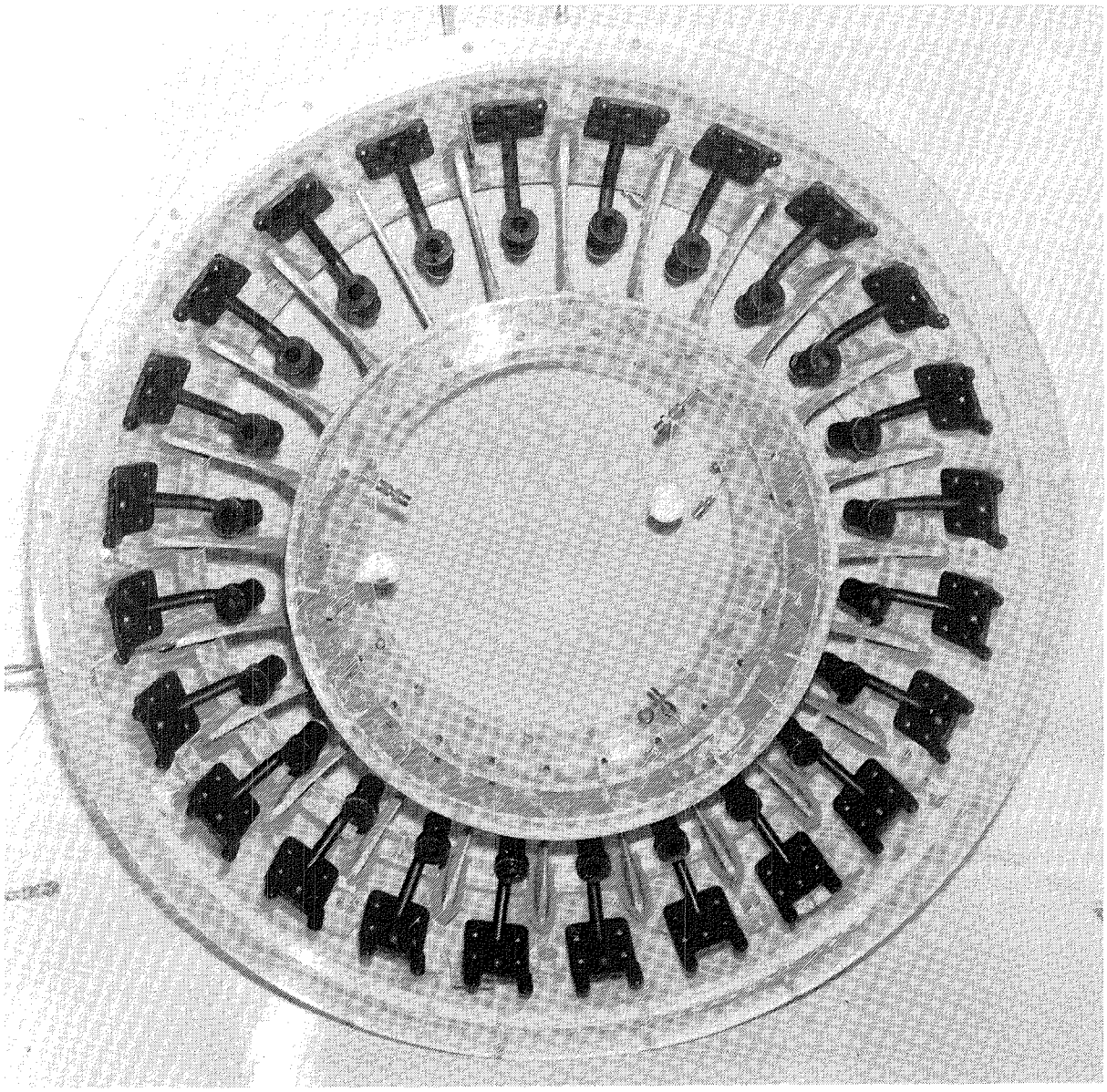

Figure 8 Definition of Geometric Characteristics - Each prediffuser wall contained a longitudinal row of seven equal-spaced static pressure taps at twelve circumferential locations.

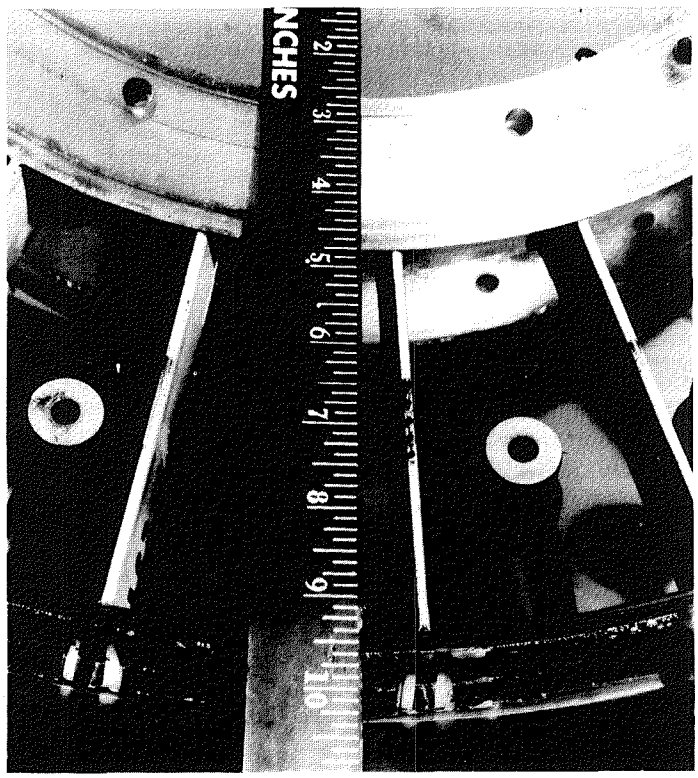

Figure 9 Diffuser Case Strut Leading Edge Total Pressure Instrumentation

The simulated combustor modules (Figures 10 and 11) comprised a hood contour mounted on a bulkhead. The bulkhead contained various hole patterns to regulate the flow in the three-branch flow system. The prediffuser exit flow is split into three streams. Two streams feed the inner and outer combustor shroud annuli, and the third supplies air to the combustor hood and pilot zone fuel nozzles (see Figure 12).

The minimum dump gap (2.85 prediffuser inlet heights) was limited by the chord length of the diffuser case struts plus additional installation tolerances to preclude contact of the hood and struts. Simulated fuel nozzle supports were also mounted in the simulated combustor modules. The instrumentation in these modules consisted of 3 static and 6 total pressure probes in the inner and outer annuli, and 3 static and 3 total pressure probes under the hood.

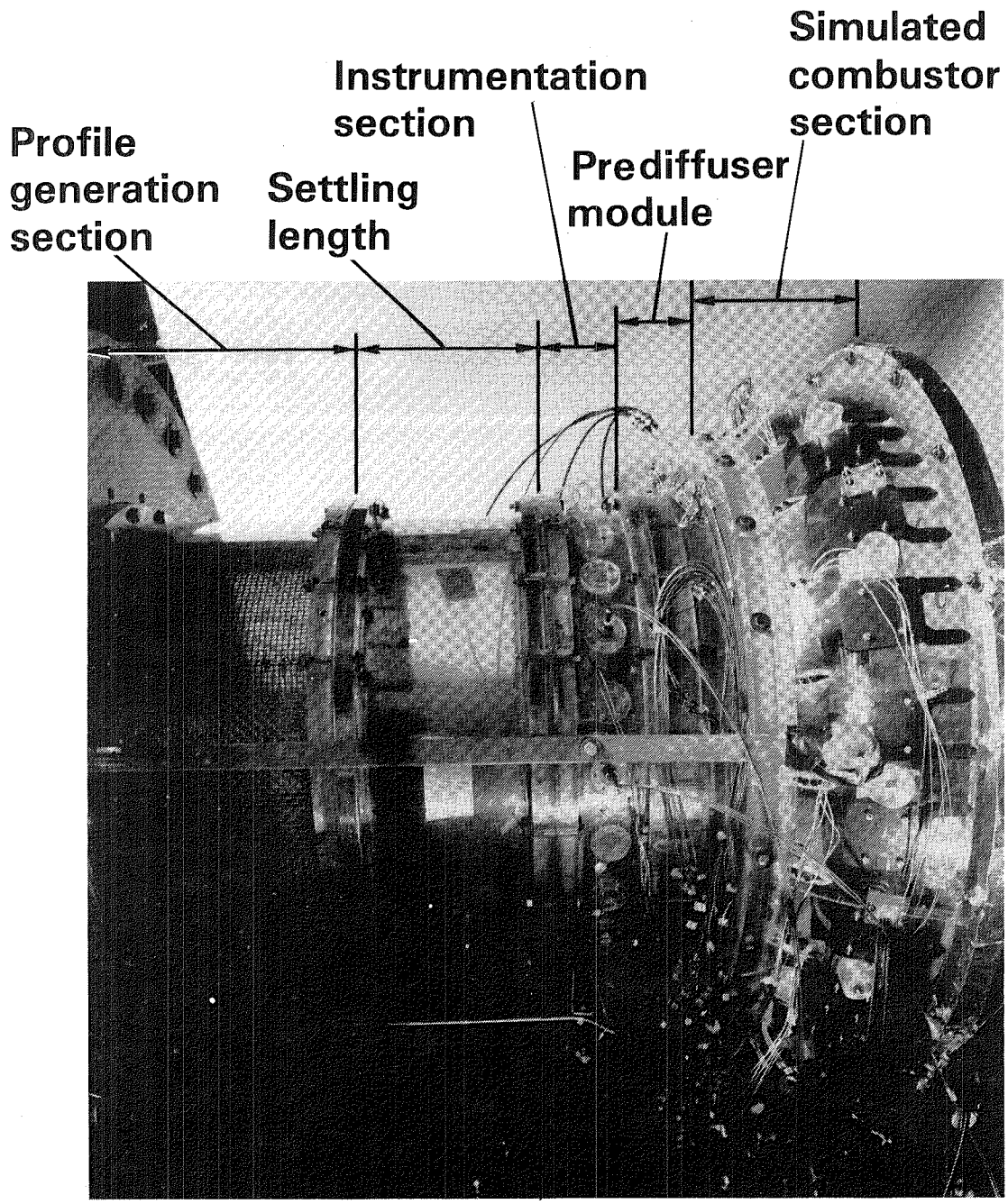

Figure 10 Side View of Baseline Prediffuser with Simulated Combustor Installed

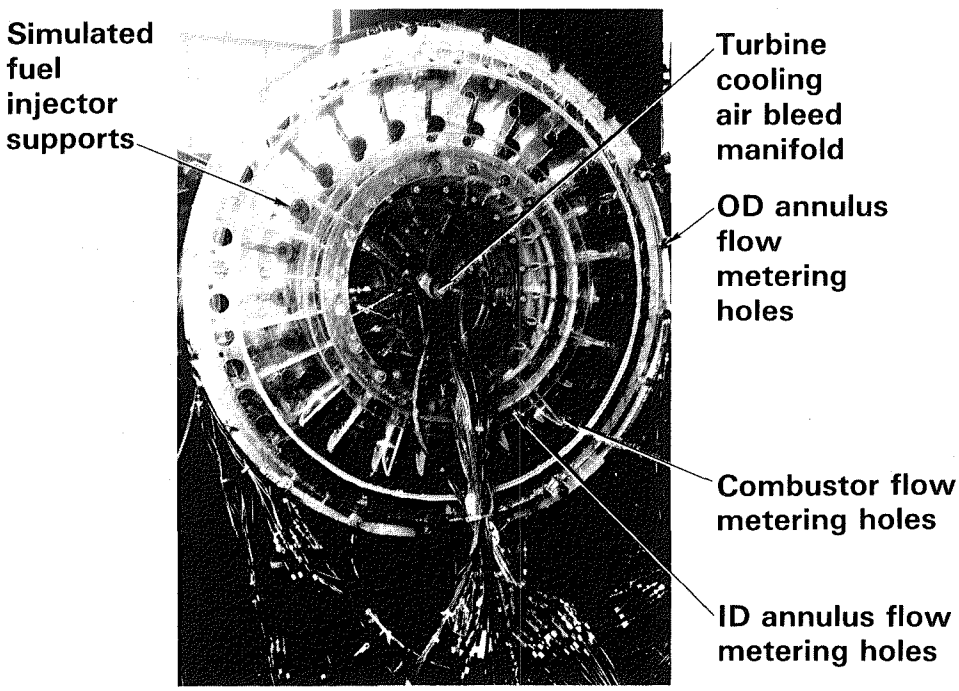

Figure 11 End View of Simulated Combustor

3.3.3.5 Full Combustor Module

The full combustor module enabled a more representative modeling of the flow area blockages in the outer annulus and of the flow supplied to the liners. The module (Figure 12) consisted of aft combustor section cases, mount pins, main zone fuel injection ports, and the complete combustor (including hood and liners). The instrumentation consisted of eight axial rows of static pressure taps with four taps per row on each case wall, and three taps per row on each liner wall. The inner and outer annuli each contained 6 four-element total pressure probes to document profiles and loss levels.

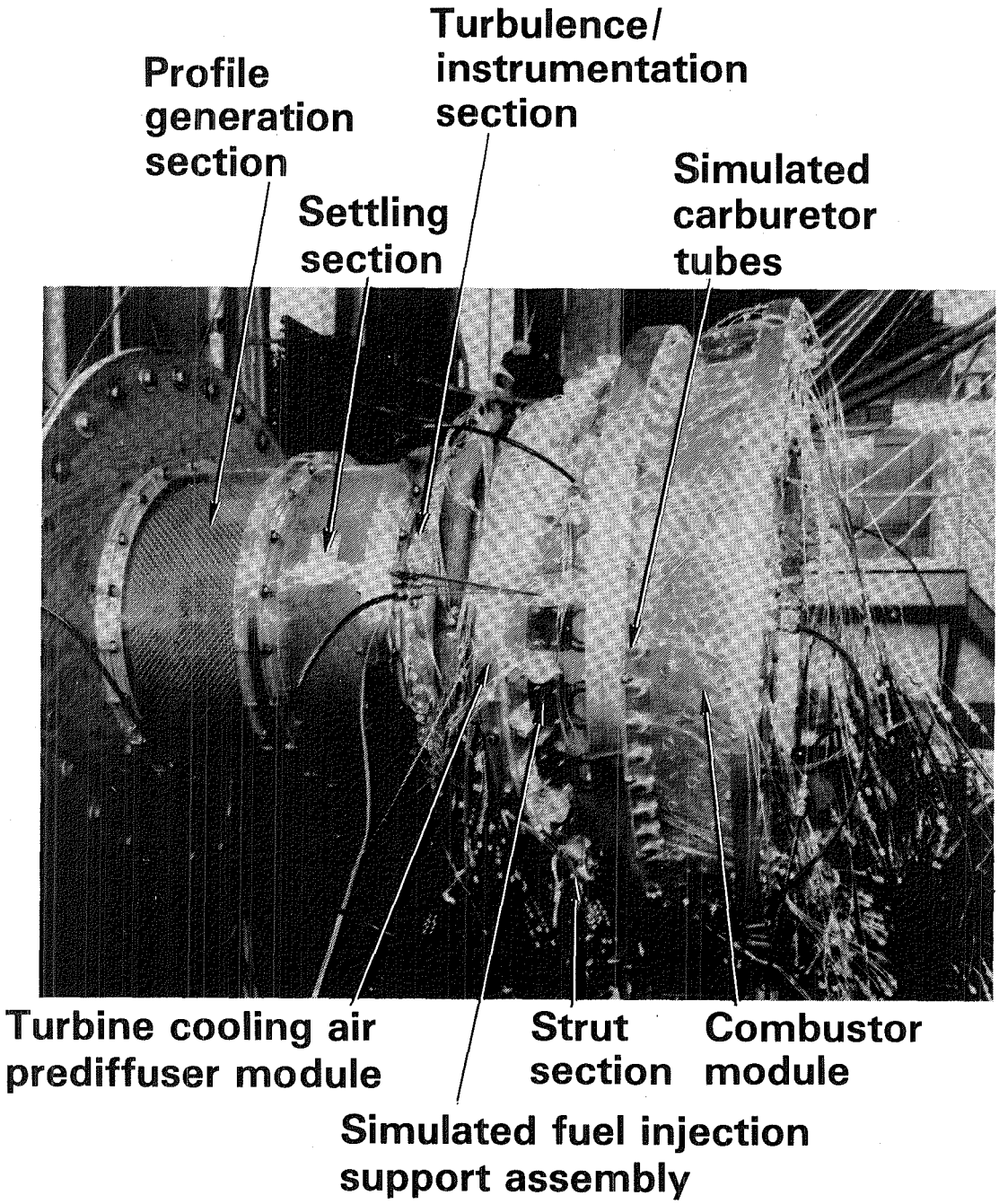

Figure 12 Rig Assembly with Full Combustor Module

3.3.3.6 Traverse Stations

Detailed total pressure radial traverses at three circumferential locations 120 degrees apart were conducted at three axial stations (see Figure 3). Pressures were measured downstream of the instrumentation section to ensure the stability of the generated profile (i.e., ensure that the radial location of the peak in the total pressure profile did not shift with axial distance). Traverses downstream of the inner wall bleed location determined the effect of

air extraction. The prediffuser exit pressure profile was documented without combustor back-pressuring to supplement measurements from fixed probes at the strut leading edge. These detailed profiles were generally measured with radially traversing miniature cobra probes. Boundary layer probes, constructed of flattened 0.38 mm (0.016 in.) hypodermic tubing, were used instead of cobra probes to define profiles near walls and near the bleed port.

3.3.4 Test Procedures

3.3.4.1 Shakedown

A rig shakedown and leakage test ensured proper instrumentation operation and eliminated any possible air leaks at rig section mating surfaces. This type of test was conducted whenever a rig configuration change took place (addition, removal, or interchange of rig sections or instrumentation).

3.3.4.2 Data Acquisition and Recording

All rig pressures were routed through scanivalves (Figure 13) employing 6.9-20.7 KPa (1-3 psi gage) transducers. These transducers transmitted the millivolt signal to an automatic data recording device (Figure 14), which stored the signal on magnetic tape for subsequent processing. All data were converted to engineering units and displayed at the test location via simultaneous transmission of the millivolt signal to a central computer. The accuracy of the individual transducers was checked by applying a known reference pressure during each scan. Frequent checks and transducer adjustments limited the measurement uncertainty to less than 0.9 percent of the prediffuser inlet dynamic pressure. The nominal value of inlet dynamic pressure was 5.5 KPa (0.8 psi) for the various configurations tested. This accuracy is reflected in a $\pm$ 0.01-degree of uncertainty in the calculated pressure rise coefficient. The same level of accuracy also applied to detailed traverse data.

3.3.4.3 Data Reduction

All test data were reduced by a computer program developed in the analysis and design phase. The program processed the raw data in engineering units and computed the parameters listed in Table 3.

TABLE 3
TEST DATA REDUCTION PARAMETERS

- Rig airflow based on orifice measurements
- Flow parameter based on measured airflow
- Flow parameter based on static and total pressures
- Mach numbers based on the two methods
- Average radial total pressure profiles
- Mass averaged total pressures
- Prediffuser pressure rise coefficients
- Total pressure loss coefficients

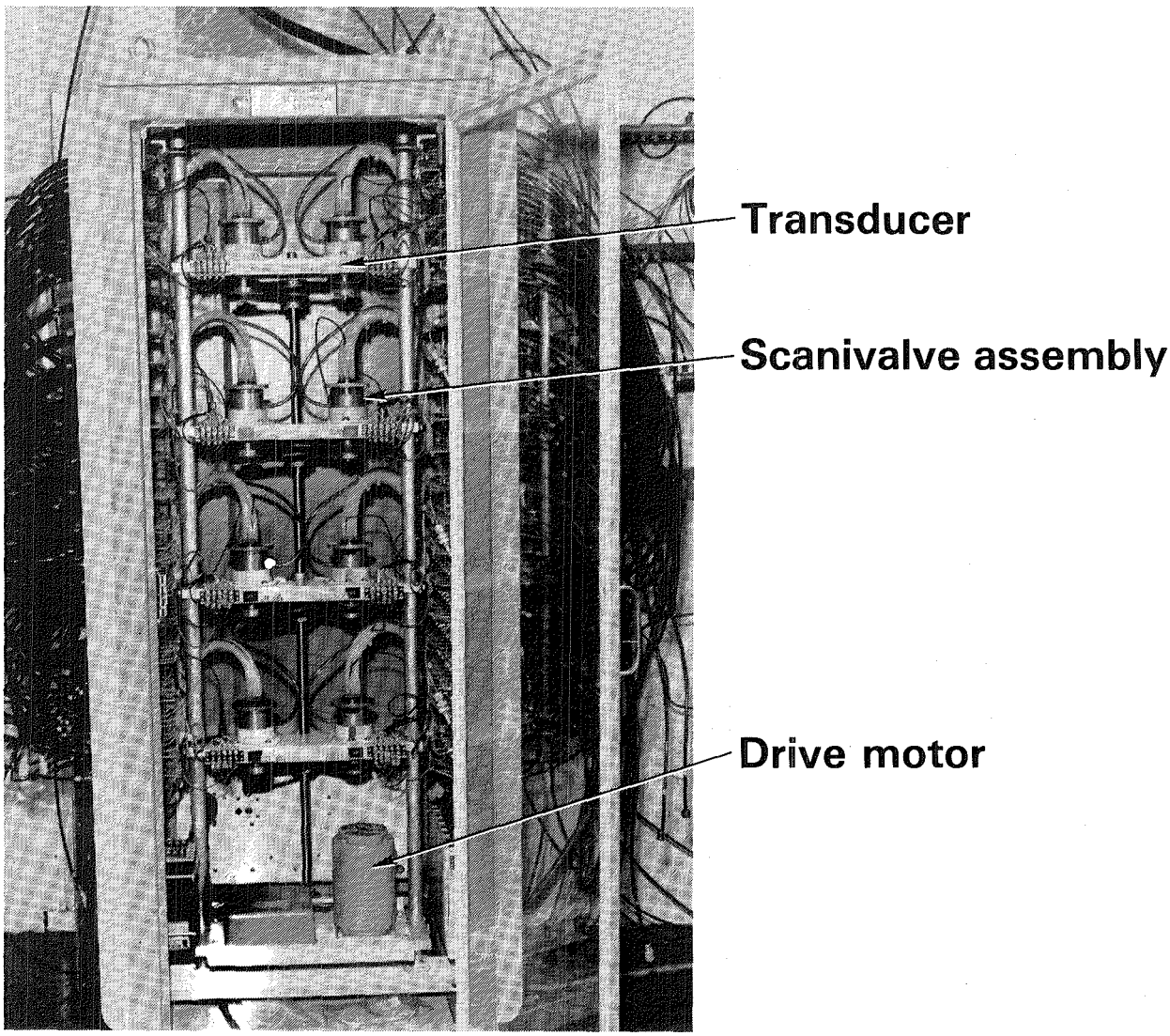

Figure 13 Scanivalve/Pressure Transducer Console

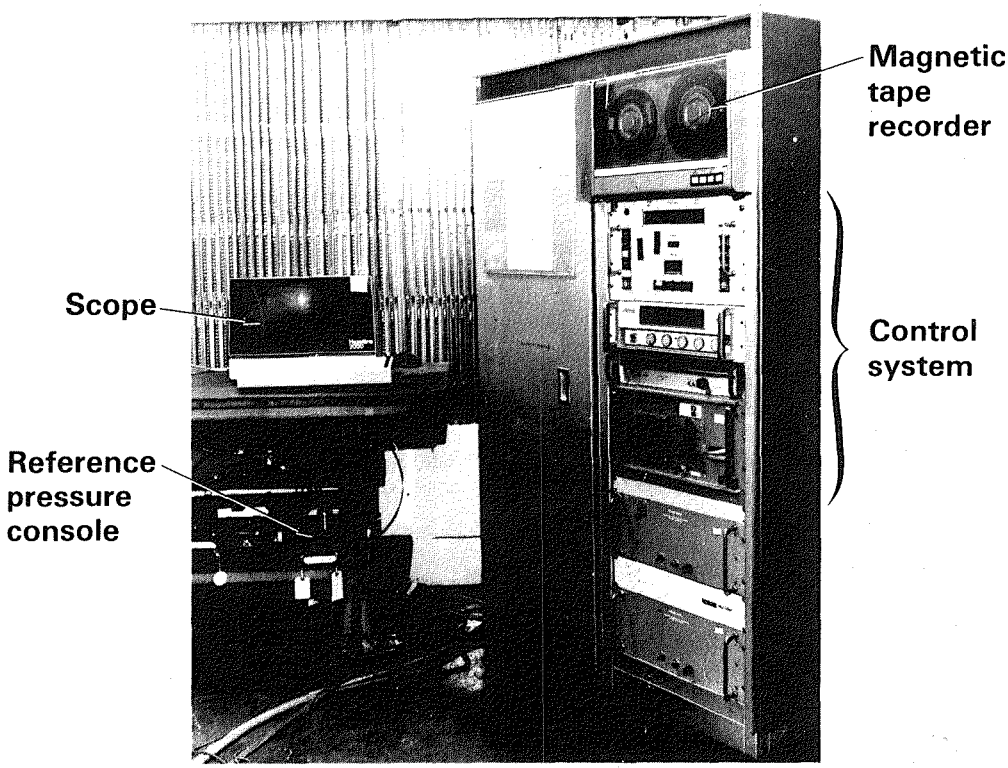

Figure 14 Automatic Data Recording System

The rig inlet and turbine cooling air bleed flow rates were calculated using the conventional orifice equation. Flow parameter based on measured airflow was calculated using Equation 1.

Equation (1)

$$FP = \frac{W_A \sqrt{T_T}}{P_S A}$$

Inlet Mach number was obtained from the flow parameter via the relationship shown in Equation 2.

Equation (2)

$$FP = \sqrt{\frac{\gamma g}{R}} \; Mn\left(1 + \frac{\gamma - 1}{2} Mn^2\right)^{1/2}$$

where $\gamma = 1.4$, $g = 32.2$ ft/sec^2, and $R = 53.3$ ft lb_f/lb_m ^oR

Wall static pressure measurements were circumferentially averaged at each axial station. Total pressure measurements at each radial location also were averaged circumferentially to obtain an average radial profile. The radial profile was integrated to obtain mass averaged value (Equations 3, 4, and 5).

Equation (3)

$$\overline{P_T} = \frac{\sum_j P_{T_j} \left(\frac{W_A}{A}\right)_j (\Delta A_j)}{\sum_j \left(\frac{W_A}{A}\right)_j (\Delta A_j)}$$

Equation (4)

$$\left(\frac{W_A}{A}\right)_j = \frac{FP_j \, \tilde{P}_{sj}}{\sqrt{T_T}}$$

Equation (5)

$$\left(\frac{P_s}{P_T}\right)_j = \left(1 + \frac{\gamma - 1}{2} M_{nj}^2\right)^{\frac{\gamma}{1-\gamma}}$$

The subscript j denotes radial location and A_j is the corresponding annular area element.

Total pressure losses to any axial station were based on the mass averaged inlet value (Equation 6).

Equation (6)

$$\lambda_{1-x} = \frac{\overline{P}_{T1} - \overline{P}_{Tx}}{\overline{P}_{T1}}$$

Static pressure recovery coefficients were calculated based on the inlet static and dynamic pressures (Equation 7).

Equation (7)

$$C_{P\ 1-x} = \frac{\tilde{P}_{sx} - \tilde{P}_{s1}}{\bar{q}_1}$$

Equation (8)

$$\bar{q}_1 = \frac{\gamma}{2} P_{s1} M_{n1}$$

3.3.4.4 Performance Tests

The test program comprised the following five phases:

Phase I - Prediffuser Inlet Flow Characterization
Phase II - Prediffuser Performance Evaluation
Phase III - Prediffuser/Combustor System Performance Evaluation
Phase IV - Sensitivity Study
Phase V - Revised Strut Evaluation.

Each of these phases is discussed in the following paragraphs.

Phase I - Prediffuser Inlet Flow Characterization

Phase I consisted of initial shakedown tests of the facility, rig, and instrumentation to ensure that each component operated properly. These were followed by a series of tests to determine the size of screens necessary to generate the required compressor exit radial total pressure profiles at the prediffuser inlet. The required profiles were based on recent experience with comparable compressors. Key considerations were the radial location of the profile peak, the circumferential uniformity of the generated profile, and the profile stability. Phase I also included measurements of turbulence levels with and without artificial turbulence generation as well as flow angle measurements of the generated swirling flows.

Phase II - Prediffuser Performance Evaluation

Phase II consisted of tests to measure the static pressure recovery of the prediffuser configurations with the prediffuser exhausting to ambient air. The total pressure profiles at the exit were measured to assess losses. These tests were conducted for various inlet profiles corresponding to those generated in Phase I. Flow visualization tests were also conducted using tufts to determine the flow stability of each configuration.

Phase III - Prediffuser/Combustor System Performance Evaluation

Phase III testing involved combining the prediffuser with either a simulated or full combustor module. The effect of hood back-pressuring on prediffuser performance was established, and total pressure losses in the three flow branches of the system were measured, either with simulated combustors or with the full combustor module.

Phase IV - Sensitivity Study

After the stability and performance evaluations of the prediffuser/combustor systems were completed, tests were conducted to determine sensitivity of the system to variations in branch flow splits, dump gap spacing, inlet profile, and air extraction at the outer wall downstream of the prediffuser dump plane.

Phase V - Revised Strut Evaluation

Structural analysis of the component diffuser case during the detailed analysis and design effort (see Figure 1) revealed that the baseline strut configuration was not adequate in carrying the case loads. A structurally adequate design with a thickened trailing edge and features that permit easy casting was subsequently designed, fabricated, and evaluated as an addendum to the diffuser/combustor model program.

Performance tests were conducted to evaluate the effect of the revised strut contour on the inner and outer shroud dump losses. Wake rake traverses were conducted on the inlet to the inner shroud. Traverses were performed behind both the baseline and revised struts employing an 11-element wake rake. A comparison of the baseline and revised strut designs is presented in Figures 15 and 16.

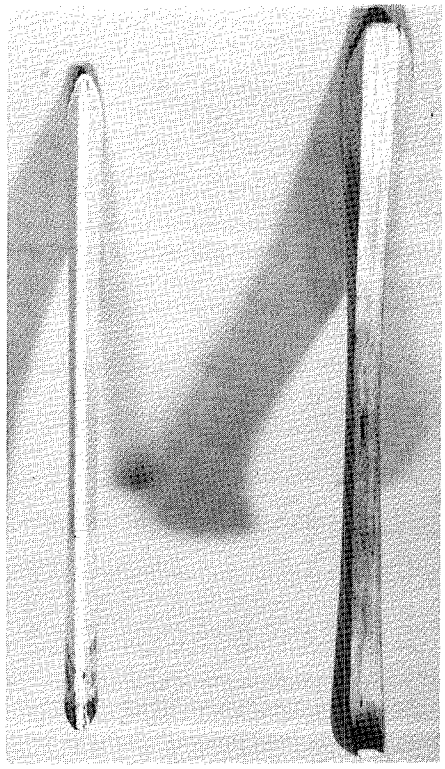

Figure 15 Comparison of the Trailing Edges of the Baseline Strut and Revised Strut Designs (view looking upstream)

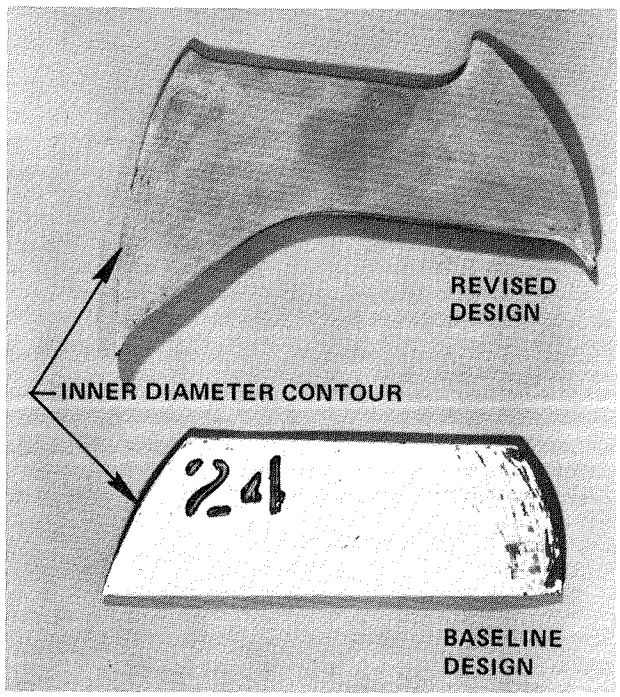

Figure 16 Comparison of the Trailing Edges of the Baseline Strut and Revised Strut Designs

4.0 RESULTS

4.1 Phase I - Prediffuser Inlet Flow Characterization

The objective of Phase I testing was to establish (within rig and test facility limitations) the flow conditions at the prediffuser inlet plane that best simulated those of a compressor discharge flow field. This effort was a technically challenging one because the typical discharge flow field exhibits significant variations in radial profile. At high power operating conditions, the circumferentially averaged radial total pressure profile is generally characterized by a peak value approximately 1 to 2 percent above the average and is located near the outer wall at 60 to 80 percent span. The tests conducted to achieve these inlet profiles are discussed in sections 4.1.1 throught 4.1.4.

4.1.1 Profile Generation

Initial testing under Phase I involved the determination of the profile delivered by the system when no particular attempt to generate a profile or to induce swirl was made. The baseline rig inlet profile is shown in Figure 17. In the region from 30 to 70 percent span, the flow exhibits a flat core where the local pressure is approximately 1 percent higher than average value (see Equation 3). The radial traverse probe data shown in Figure 17 is taken three annulus heights downstream of the stationary probes.

Figure 18 shows the circumferential uniformity of the center peaked profile as measured at the instrumentation section. At any spanwise location, the local total pressure deviated from the circumferential average at that span within 0.5 percent of the mass average inlet total pressure.

Generation of Outer Diameter Peaked Profile. Generation of an outer diameter peaked profile was originally attempted using one layer of wire screen 0.64 cm (0.25 in.) square mesh of 0.16 cm (0.062 in.) wire) on the inner diameter wall of the profile section immediately upstream of the instrumentation section. The resultant profile (Figure 19) is clearly shifting (i.e., unstable) as it travels axially. This is evidenced by the difference between the stationary and traverse probe profiles. A smooth wall annular duct was inserted between the profile generation and instrumentation sections to dampen the nonequilibrium forces produced by the wire screen. The process of profile generation followed by settling length yielded the profile shown in Figure 20. This profile is acceptable as a simulation of the compressor exit profile at engine high power operating conditions. It exhibits a 1.5 percent peak-to-average pressure at approximately 65 percent span location. The circumferential uniformity of the stable outer diameter peaked profile is shown in Figure 21. At any spanwise location, the local total pressure deviated from the circumferential average at that span by less than 2 percent of the mass average inlet value.

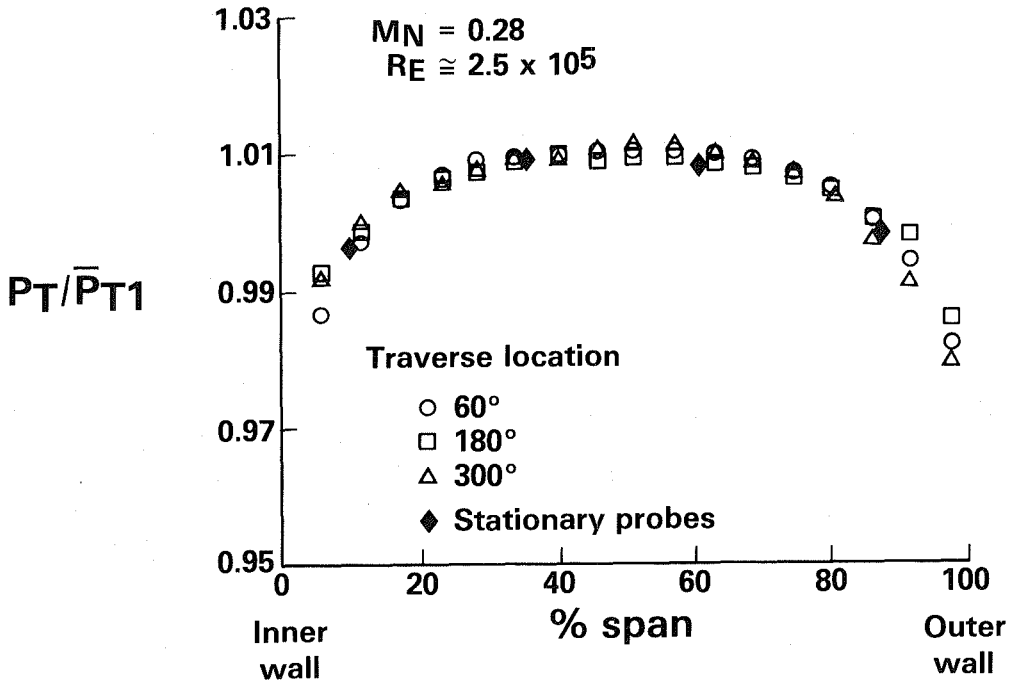

Figure 17 Center-Peaked Inlet Profile

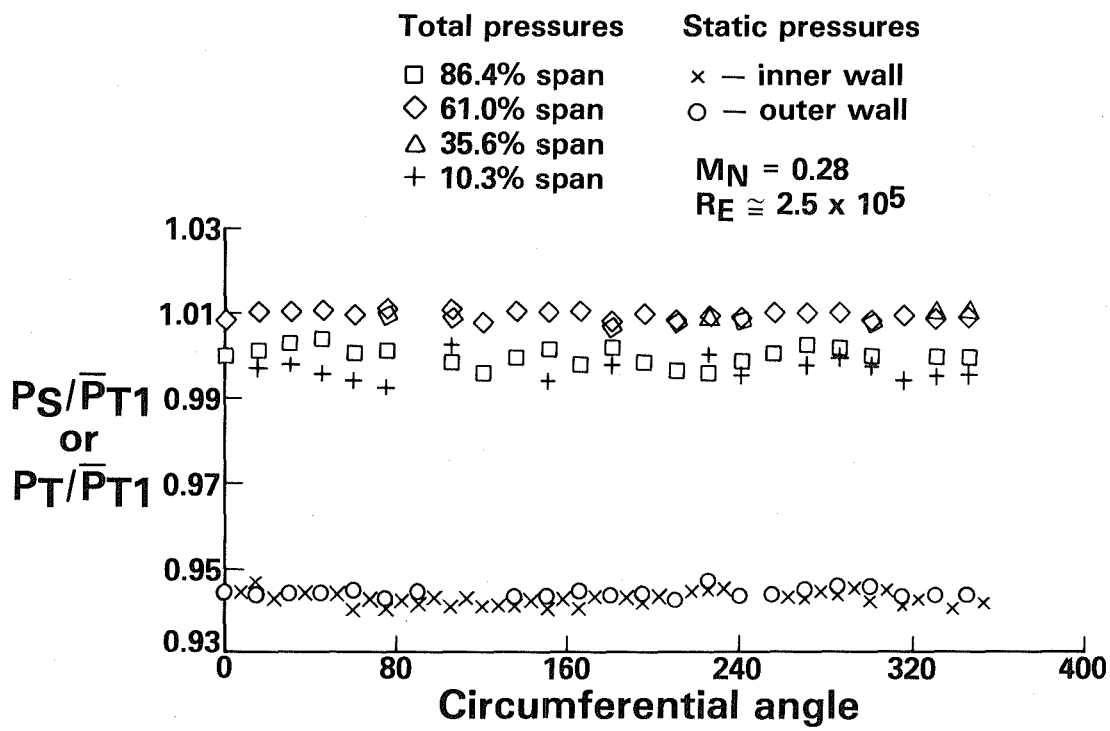

Figure 18 Circumferential Uniformity of Center-Peaked Inlet Profile

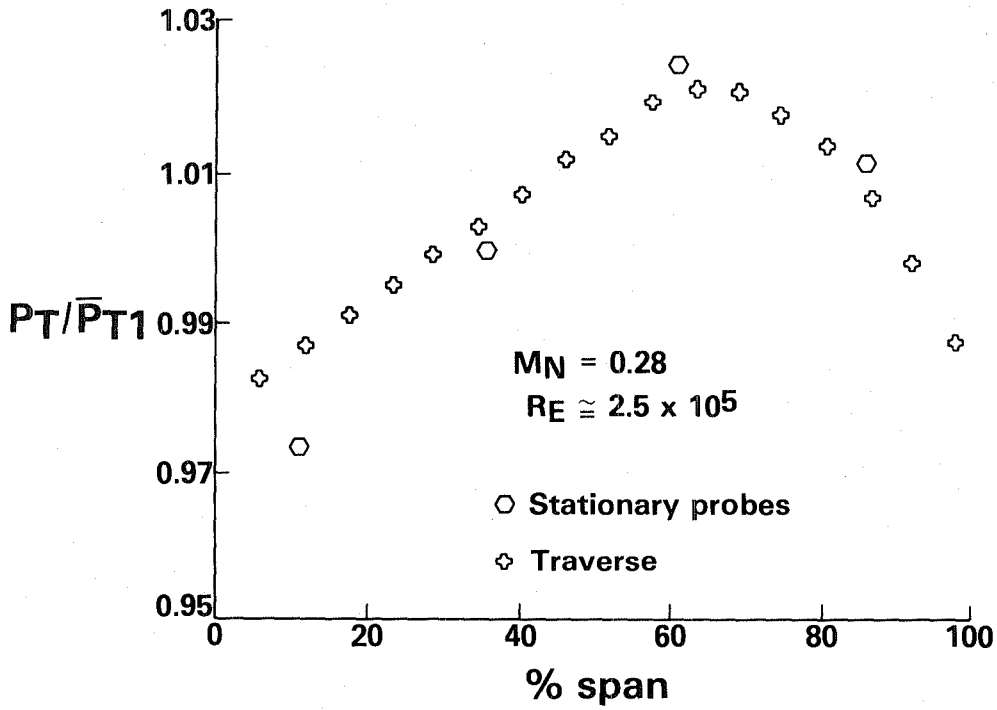

Figure 19 Unstable Outer Diameter Peaked Profile

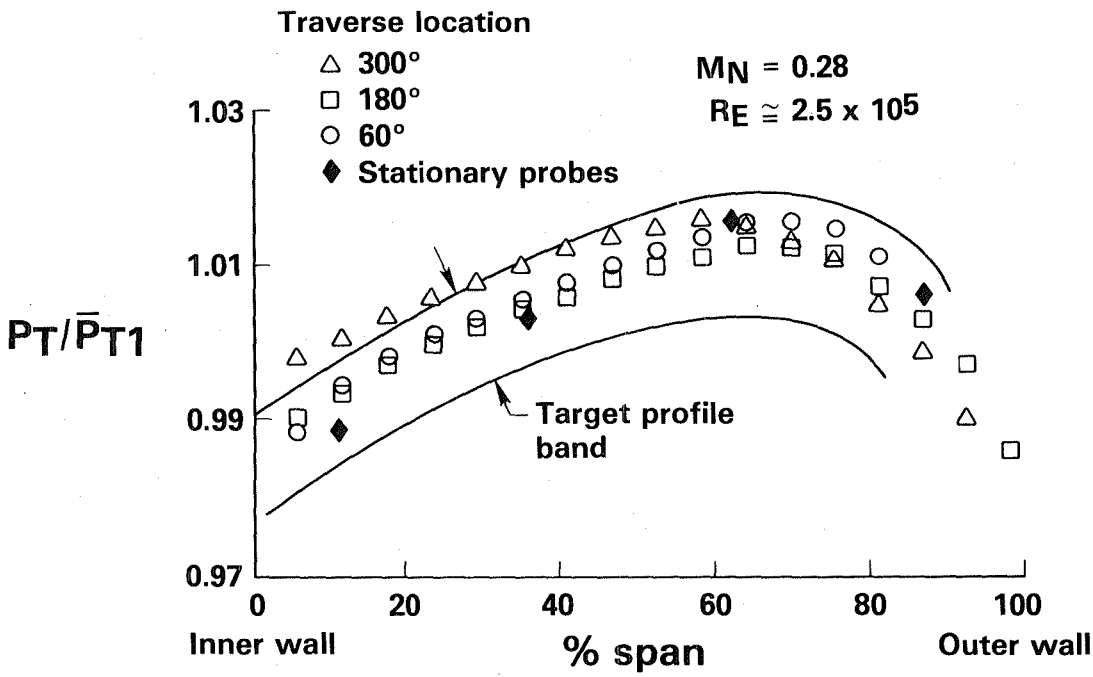

Figure 20 Stable Outer Diameter Peaked Profile

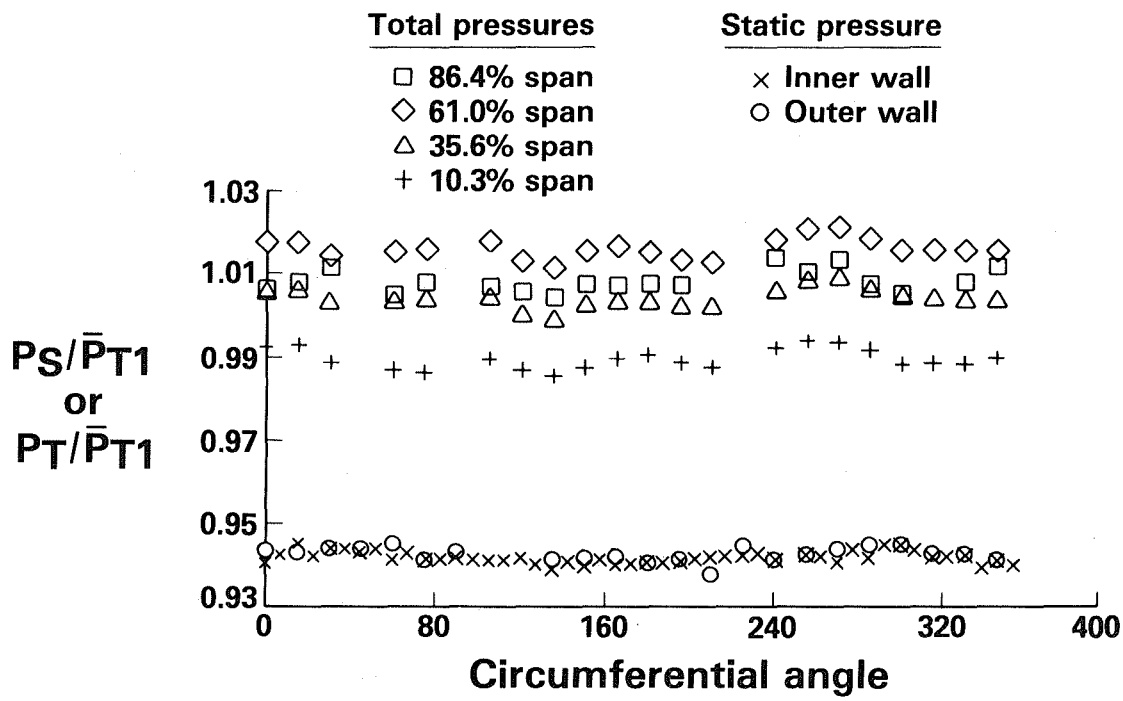

Figure 21 Circumferential Uniformity of the Stable Outer Diameter Peaked Profiles

Generation of Inner Diameter Peaked Profile. An attempt to generate an inner diameter peaked profile was conducted using one layer of screen on the outer wall of the profile section, followed by the same settling length discussed previously. The generated radial total pressure profile is shown in Figure 22. The profile is peaked at approximately 35 percent span. A comparison of stationary versus traverse profile indicates a stable profile has been generated. The circumferential uniformity characteristics of the inner diameter peaked profile were very similar to the outer peaked one.

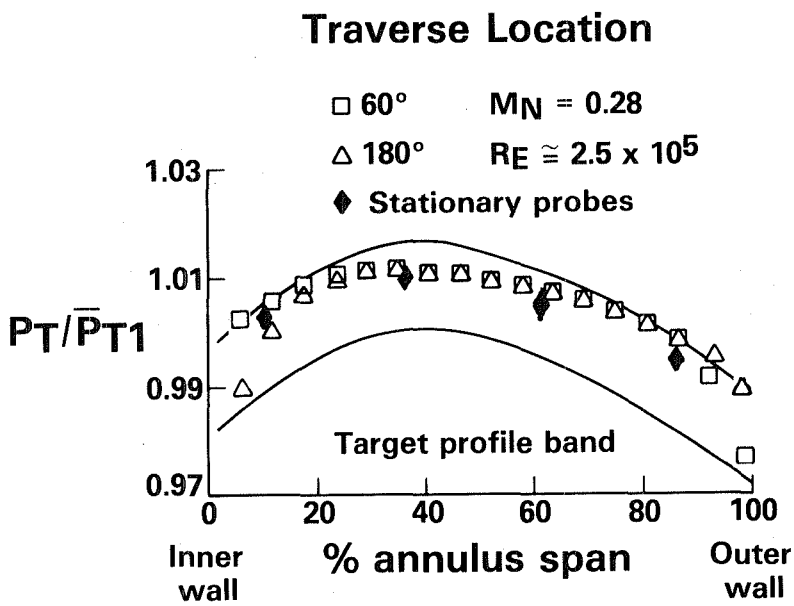

Figure 22 Inner Diameter Peaked Profile

4.1.2 Turbulence Intensity

Based on engine test data (reference 1) a target core turbulence intensity level of 6 to 7 percent at the prediffuser inlet plane was chosen for the test program. Tests were conducted to determine the rig turbulence characteristics. Initially, a rig baseline test was conducted using only the inlet section with no screen attachment. The baseline rig turbulence intensity profile is shown in Figure 23. The core value was approximately 2 percent. The desired level of 6 to 7 percent was achieved by placing a coarse mesh wire screen (48 percent flow blockage) normal to the flow field upstream of the instrumentation section (see Figure 3). The resultant turbulence intensity profile is shown in Figure 23 and exhibits a core value of approximately 5 to 7 percent. Measurements of turbulence characteristics with an outer diameter peaked profile in conjunction with the turbulence generation showed an overall

increase in the core of 1 to 2 percent with larger increases nearer the walls. The larger turbulence intensity level near the inner diameter wall is caused by the effects of the upstream profile generation screen attached to the inner wall. It was determined that the turbulence generating screen attenuated the total pressure profile peak by approximately 0.1 percent, which was considered negligible.

4.1.3 Turbine Cooling Air Bleed Simulation

Tests were conducted to determine the influence of extracting up to 3.5 percent of the inlet flow from the inner wall just upstream of the 5-degree outboard cant in the compressor exit guide vane section. The 3.5 percent level is predicated by turbine cooling requirements. The resultant effect on the prediffuser inlet profile is shown in Figure 24. The traverse data were taken at a plane corresponding to the exit area of the compressor exit guide vane. The test was conducted for the outer diameter peaked profile with axial flow only; hence, the compressor exit guide vane assembly was replaced with the assembly containing only the support struts. The effect on air extraction was localized between the inner wall and 15 percent span and did not affect the spanwise location or magnitude of the total pressure peak (see Figure 24).

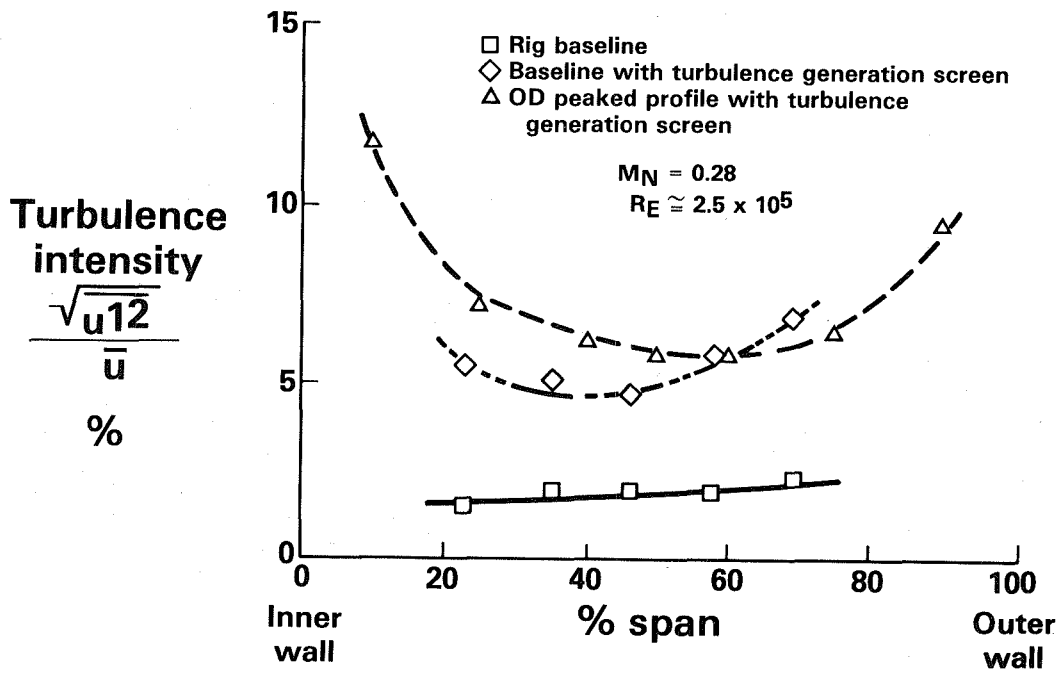

Figure 23 Turbulence Intensity Characteristics at Prediffuser Inlet

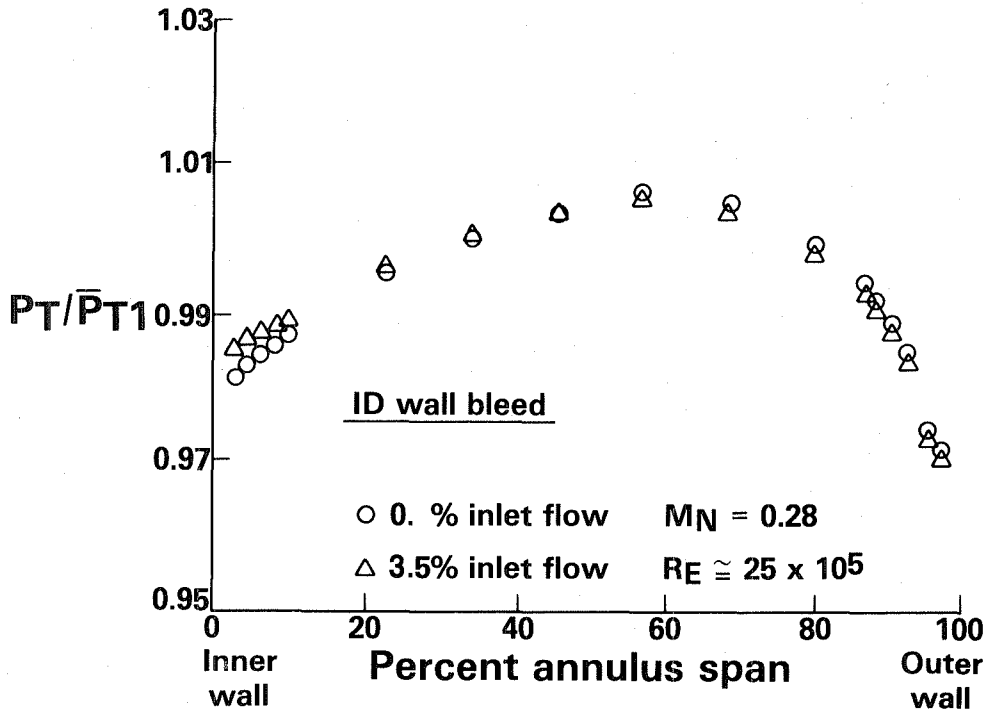

Figure 24 Effect of Turbine Cooling Air Bleed on Inlet Profile

4.1.4 Swirl Generation

The Phase I results discussed in sections 4.1.1 through 4.1.3 were all obtained with axial flow. The remainder of Phase I testing consisted of attempts to integrate swirl generation capabilities into the rig inlet module. The intent was to impart enough swirl to the flow so that the compressor exit guide vane operation would be properly simulated. Then, the flow at the prediffuser inlet, and the secondary flows and wakes resulting from the exit guide vanes would exhibit the desired velocity profile. Several problems were encountered during this testing. Each section of the rig inlet module contained, at the upstream and downstream end, 6 axial support struts that maintained the proper annulus spacing in the sections. These struts generated wakes which quickly dissipated in the axial flow case. In the swirling flow case, however, the incident flow angle on the struts generated wake regions which significantly undermined the circumferential uniformity of the flow field.

The most serious problem was the generation of swirl in conjunction with a radial profile. When the profile was generated and passed through the swirl section, the intense mixing caused by the preswirl vanes eliminated the characteristics of the profile. The final profile was essentially center peaked for all profile generation methods and displayed a high degree of circumferential nonuniformity. When the swirl generation section was installed upstream of the profile generation and settling sections, the profile did not achieve the desired inner or outer peakedness ($\sim$ 1.5 percent). This was caused primarily by the back-pressuring effect of the exit guide vane assembly. Elimination of the settling length to achieve a higher peak-to-average profile generated a highly unstable profile (i.e., the location and magnitude of the peak changed with axial distance).

Test facility inlet pressure limitations, coupled with limitations of the rig hardware, made it impossible to generate profiles with swirl that exhibited the desired shape, stability, and circumferential uniformity. The inability to properly measure the aerodynamic performance of the combustor section with swirling inlet flow resulted in the elimination of preswirl/exit guide vane assembly from the test program.

These limitations imposed a certain degree of conservatism in the stability evaluation of the prediffusers, since the increased turbulence levels and intense mixing resulting from the compressor exit guide vanes were not present. Such a flow field would tend to retard flow separation in an adverse pressure gradient field. The absence of the vanes was not expected to influence the system performance, as evidenced by other investigations (references 2 and 3). Therefore, it was decided to remove the swirl generation/compressor exit guide vane hardware from the subsequent test program in order to ensure stable, relatively uniform, and, hence, well-defined inlet flow characteristics to the prediffusers. This would improve the validity of performance measurements and sensitivity studies.

The prediffuser inlet flow conditions in Table 4 were established as representative baseline values and were employed in the prediffuser and overall system performance evaluation tests, unless otherwise stated.

TABLE 4

BASELINE PREDIFFUSER MODULE INLET FLOW CHARACTERISTICS

Profile Shape	1.1-1.5% peak-to-average P_{T1}
Position of Peak	60-65% of span
Profile Energy Coefficient,	1.093
Blockage Parameter, B_1	0.11
Mean Inlet Mach Number	0.28
Core Turbulence Intensity	6-7%
Reynolds Number	2.5×10^5
Nominal Inner Wall Bleed	3.5% of inlet flow

4.2 Phase II - Prediffuser Performance Evaluation

The performance evaluation conducted in this phase included flow visualization tests, prediffuser exit total pressure traverses, and evaluation of the static pressure recovery characteristics. All tests were conducted with inner diameter, center, and outer diameter peaked inlet profiles and with no combustor hardware downstream of the prediffuser exit.

Flow visualization tests were conducted with wool tufts attached to the prediffuser inner and outer walls in a random pattern, providing a good coverage of the full circumference. A tufted wand was also used to conduct local investigations near the exit plane.

All three prediffuser configurations (see Figure 4) were evaluated first with the baseline inlet conditions as generated in Phase I (see Table 4). The prediffuser inlet and exit total pressure profiles without back-pressuring by the combustor hood are shown in Figure 25. The total pressure profiles for all configurations adjust from the highly peaked outer diameter inlet profile to an exit profile, which is peaked at approximately the center of the duct. Wall tufts indicated no flow separation in any of the three configurations for an outer diameter peaked inlet profile. The short prediffuser (configuration III) exhibited lower total pressure and lower velocity near the outer wall, which indicated less margin to flow separation than with configurations I and II (see Figure 25). In fact, it was noted that local flow separation could be induced in prediffuser III by slightly increasing the wake region behind probes upstream of this prediffuser. The flow was not separated at any other circumferential position.

The axial wall static pressure recovery characteristics of the prediffuser configurations without backpressuring are shown in Figure 26. For an outer diameter peaked profile, the average exit plane value of the static pressure recovery coefficient (C_p) corresponds to diffuser efficiencies of 64, 68, and 64 percent for configurations I, II, and III, respectively. The reduced pressure on the outer wall is caused by local acceleration of the flow as it is turned outboard on this wall.

Subsequent testing was conducted in this phase of the program to investigate flow stability and to measure the performance of the three configurations with center and inner diameter peaked inlet total pressure profiles as generated in Phase I. The inlet and exit total pressure profiles for the three prediffusers are shown in Figure 27 for the center peaked inlet profile case. The exit profile exhibits a peak at the center of the duct for configurations I and III, but the exit profile of configuration II is peaked at slightly less than 50 percent span. The axial wall static pressure recovery characteristics for a center peaked inlet profile are shown in Figure 28. The exit plane values correspond to efficiencies of 60, 64, and 60 percent for configurations I, II, and III, respectively. All three prediffusers were observed to operate separation-free for the center peaked profile.

The results of performance evaluation tests of each configuration with an inner diameter peaked inlet profile are shown in Figures 29 and 30. The prediffuser exit total pressure profile (Figure 29) shows no change in the radial position of the peak from inlet to exit. Exit plane efficiencies were 64, 66, and 61 percent for configurations I, II, and III, respectively. All three configurations were found to be separation free with an inner diameter peaked inlet profile. The values of exit recovery coefficients for all three configurations with the three inlet profiles are summarized in Table 5.

TABLE 5

PREDIFFUSER PERFORMANCE WITH NO BACK-PRESSURING

Inlet Profile	OD Peaked			Center Peaked			ID Peaked		
Configuration	$\widetilde{C}_{P1-2}$	$\widetilde{\eta}$	$\bar{M}_{n2}$	$\widetilde{C}_{P1-2}$	$\widetilde{\eta}$	$\bar{M}_{n2}$	$\widetilde{CP}_{1-2}$	$\widetilde{\eta}$	$\bar{M}_{n2}$
I	0.36	0.64	0.179	0.34	0.60	0.186	0.36	0.64	0.174
II	0.41	0.68	0.168	0.38	0.64	0.169	0.39	0.66	0.168
III	0.36	0.64	0.179	0.34	0.60	0.179	0.34	0.61	0.181

4.3 Phase III - Prediffuser/Combustor System Performance Evaluation

In this phase of the program, the performance of each prediffuser configuration with downstream combustor hardware was evaluated. The baseline combustor test conditions, for flow split and dump gap employed in this series of tests, correspond to those summarized in Table 6. Results are reported for tests employing the baseline strut design, unless otherwise noted.

TABLE 6

BASELINE COMBUSTOR CONDITIONS

Dump Gap Spacing ($X/\Delta R$)	2.85
Inner Annulus Flow ($\%W_{a2}$)	20.7
Outer Annulus Flow ($\%W_{a2}$)	60.6
Hood Flow ($\%W_{a2}$)	18.7

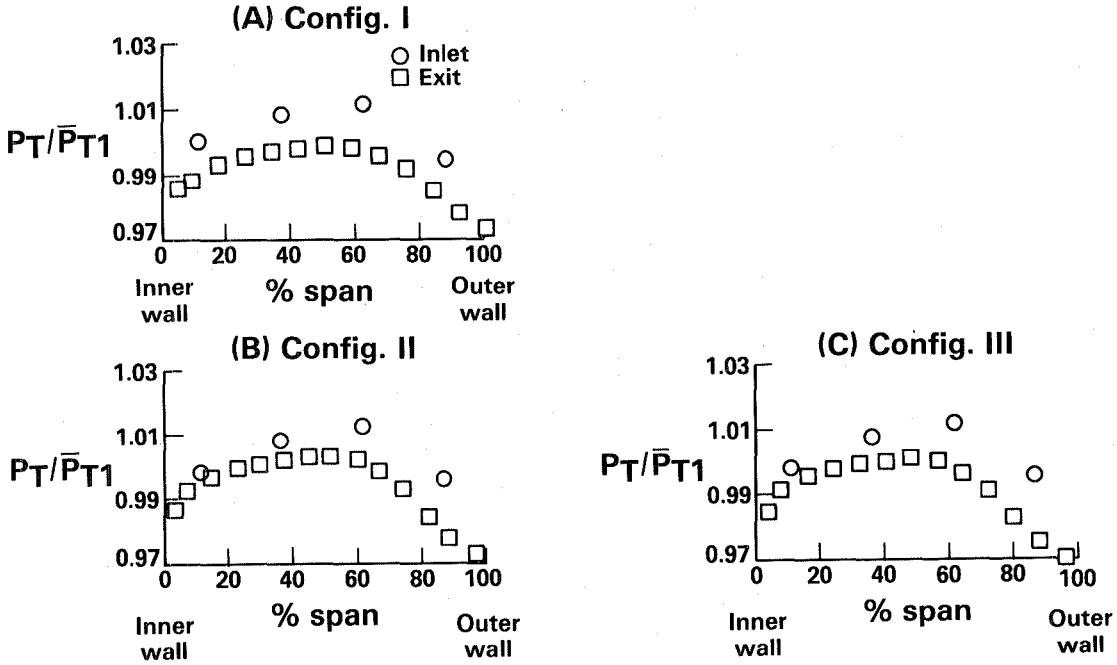

Figure 25 Inlet and Exit Total Pressure Profiles for Three Prediffuser Configurations Evaluated with an Outer Diameter Peaked Inlet Profile and No Back-Pressuring

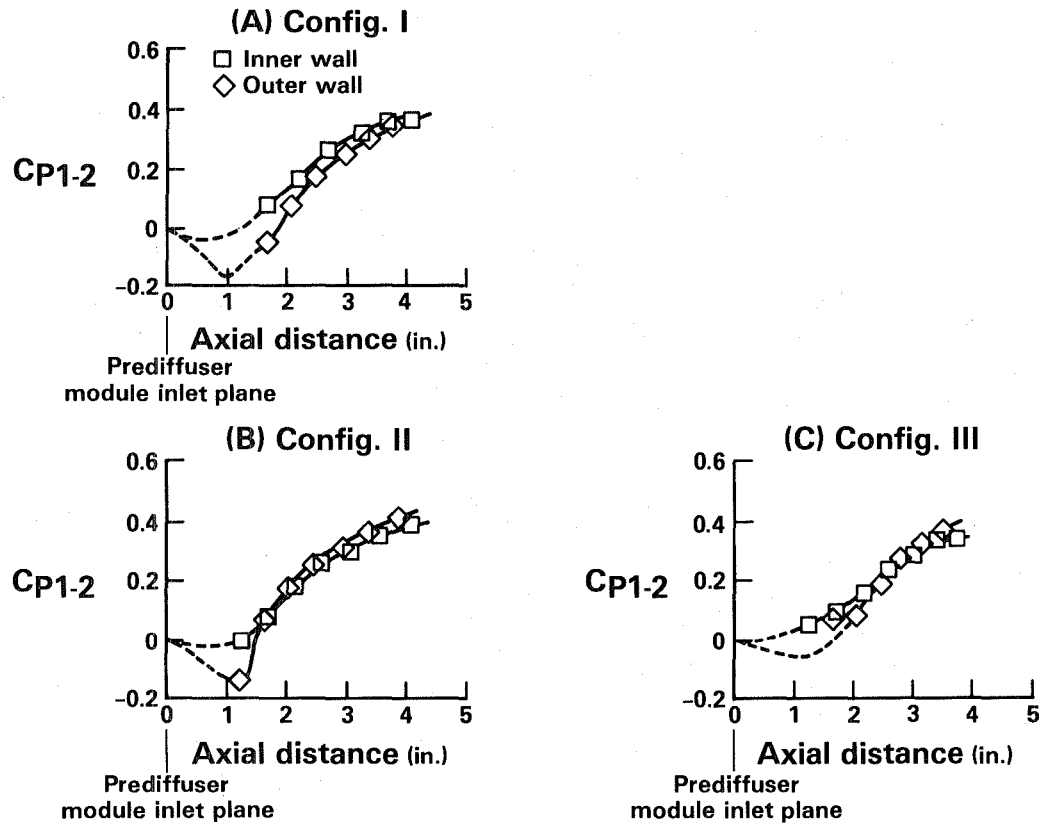

Figure 26 Static Pressure Recovery Distributions for Three Prediffuser Configurations Evaluated with an Outer Diameter Peaked Inlet Profile and No Back-Pressuring

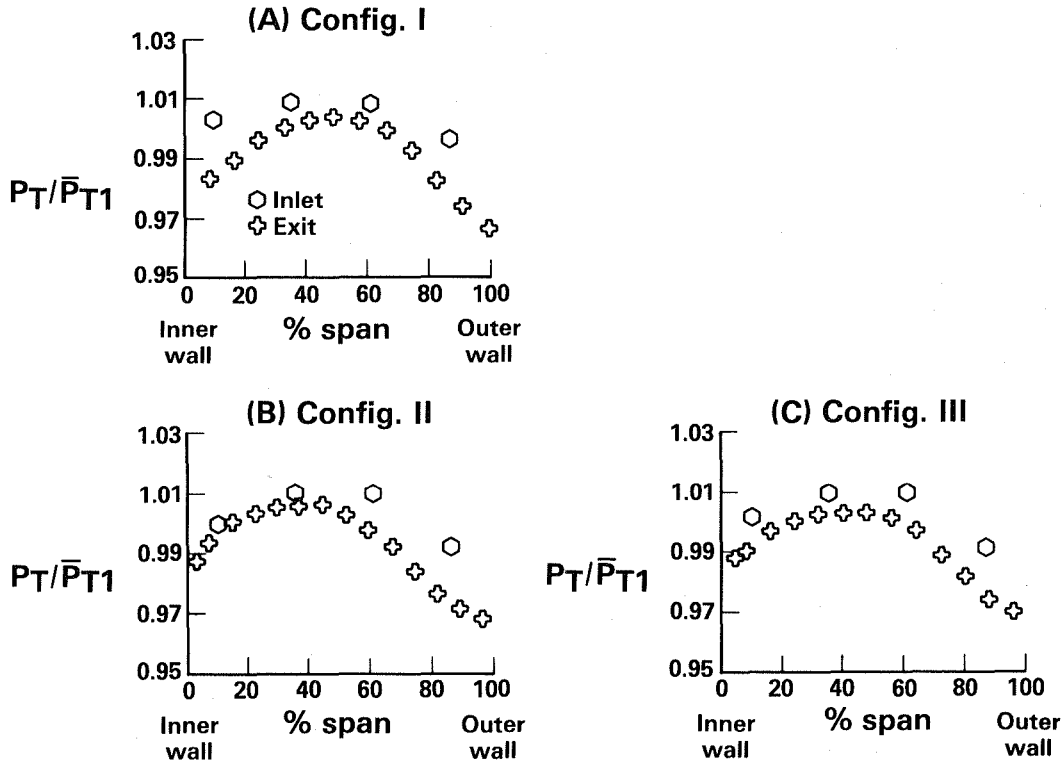

Figure 27 Inlet and Exit Total Pressure Profiles for Three Prediffuser Configurations Evaluated with a Center Peaked Inlet Profile and with No Back-Pressuring

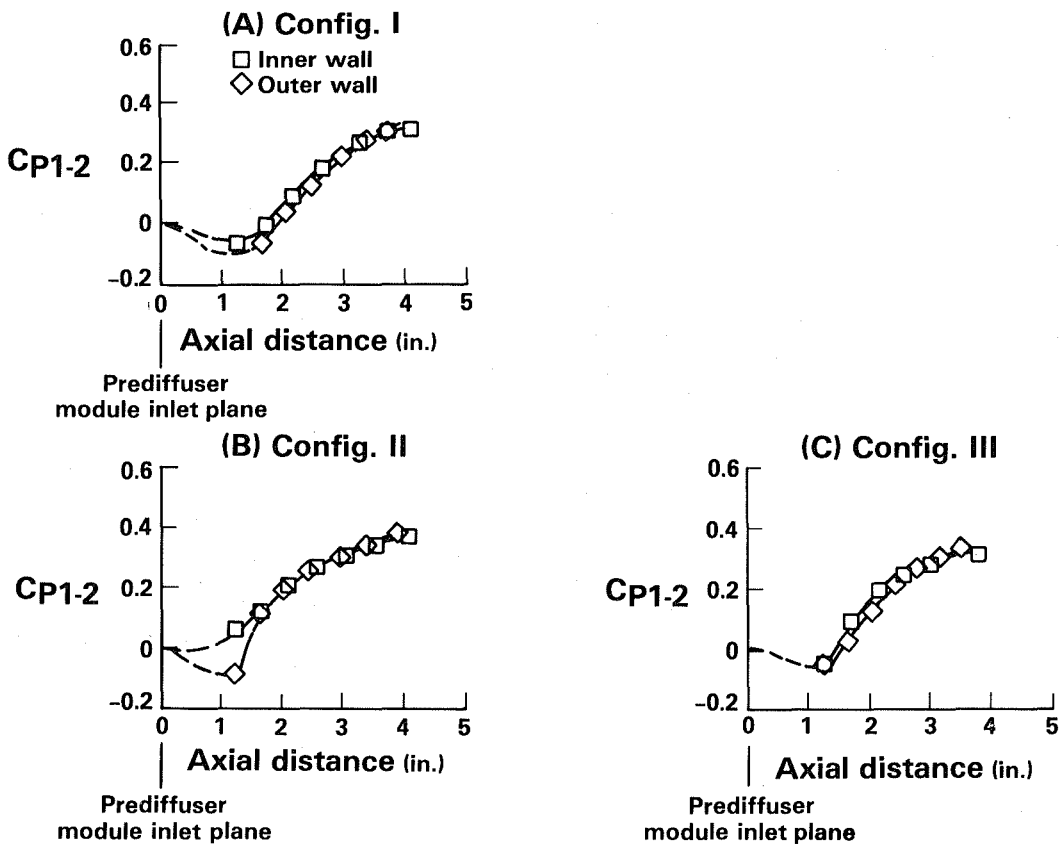

Figure 28 Static Pressure Recovery Distributions for Three Prediffuser Configurations Evaluated with Center Peaked Inlet Profile and No Back-Pressuring)

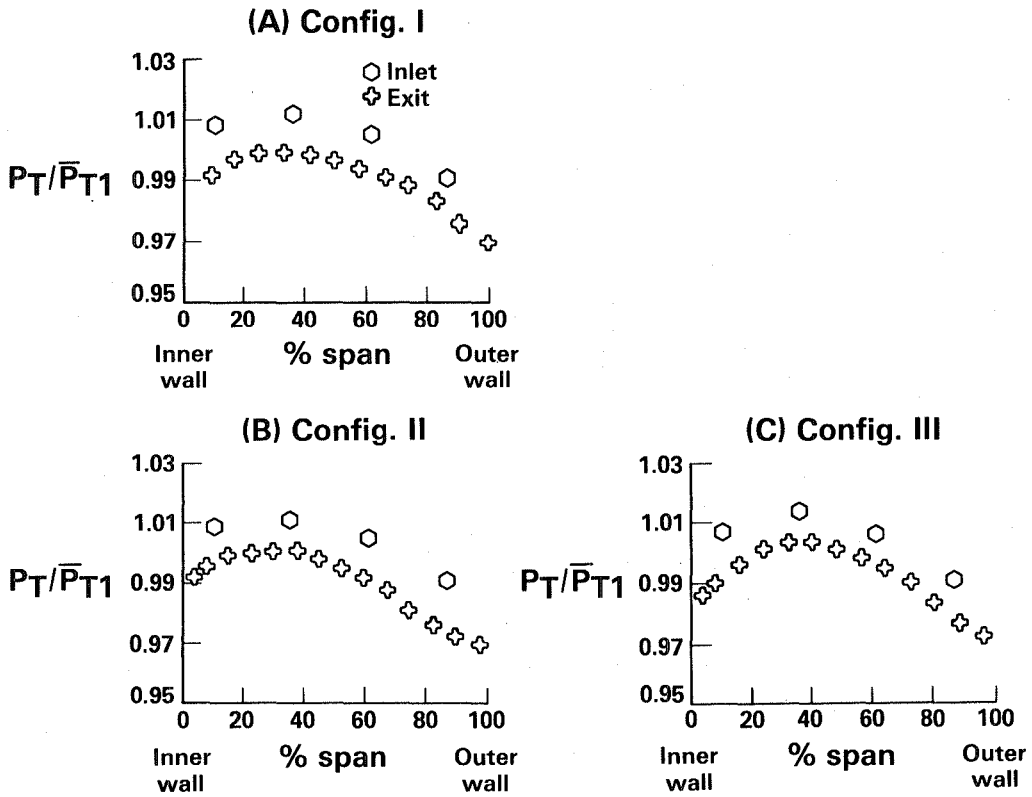

Figure 29 Inlet and Exit Total Pressure Profiles for Three Prediffuser Configurations Evaluated with an Inner Diameter Peaked Inlet Profile and No Back-Pressuring

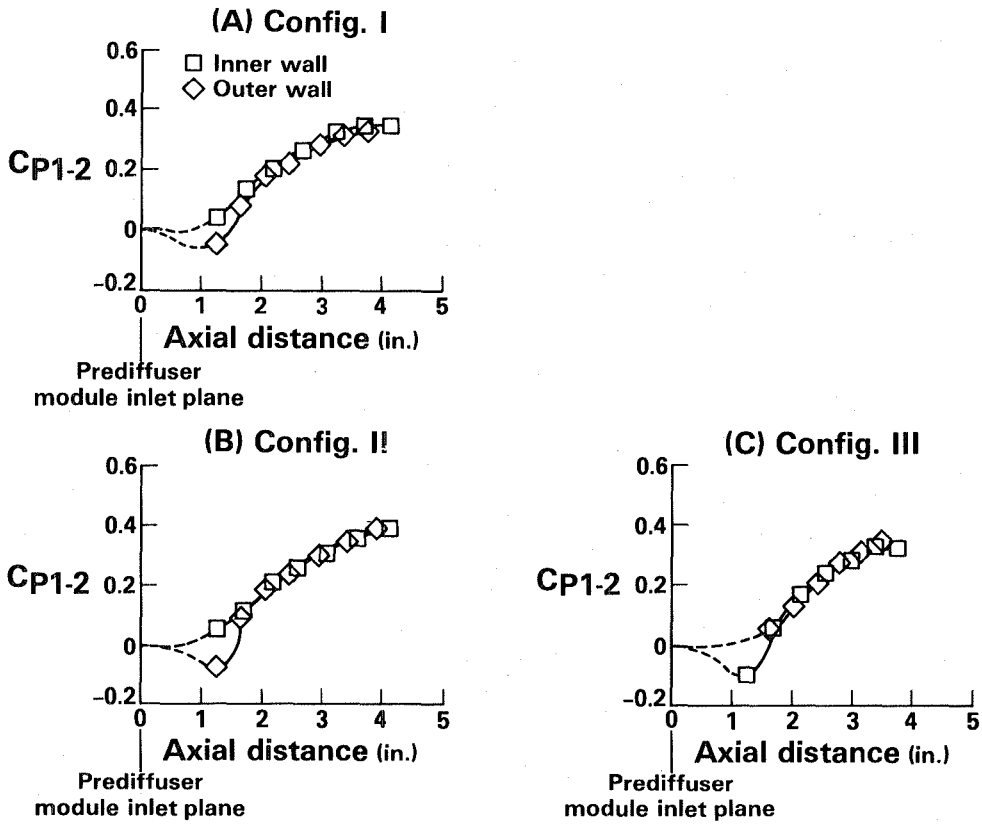

Figure 30 Static Pressure Recovery Distributions for Three Prediffuser Configurations Evaluated with an Inner Diameter Peaked Inlet Profile and No Back-Pressuring

4.3.1 Hood Back-Pressuring

The prediffuser inlet and exit total pressure profiles, with and without the back-pressuring influence of the combustor hood, are presented in Figure 31. The inlet profile with the combustor installed has been omitted for clarity because the shape of the radial pressure profile was not influenced by the presence of a combustor hood for $X/\Delta R = 2.85$ and larger. The results of hood back-pressuring tests indicate that back-pressuring contributed to reduced losses in the 40 to 100 percent span region and had a negligible effect on the inner diameter portion of the exit profile (0-40 percent span). The exit profile for the back-pressured case shows that the total pressure distributions for all configurations adjust to an exit profile peaked at the center of the duct. This is also true for the prediffusers exhausting to an ambient atmosphere.

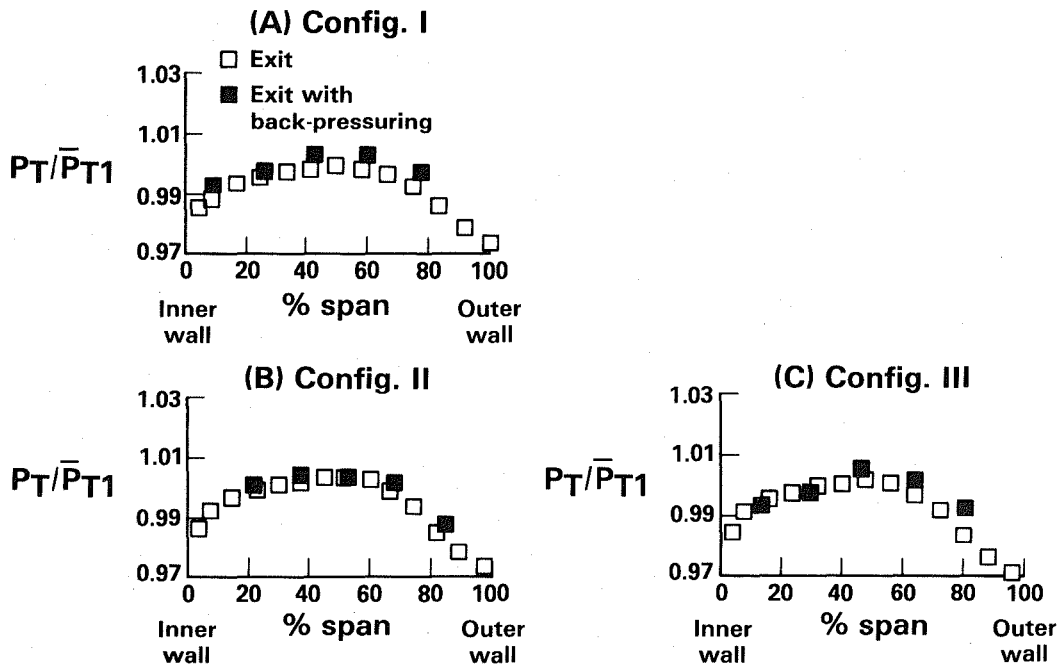

Figure 31 Effect of Back-pressuring on Outer Diameter Peaked Inlet Profile

The axial diffusion characteristics when each prediffuser is coupled to its respective simulated combustor module are presented in Figure 32. Comparison of Figures 32 and 26 shows that the pressure recovery coefficient on the inner wall of all three prediffuser configurations increased with the combustor present. The outer wall pressure recovery was reduced because the combustor flow distribution required approximately 60 percent of inlet flow in the outer shroud annulus. This highly biased flow split induced streamline flow curvature and acceleration, which is reflected in reduced pressure recovery over the downstream half of the outer wall of each prediffuser.

The overall performance characteristics of the prediffuser/combustor systems are summarized in Table 7. The pressure rise and total pressure loss coefficients are presented for both the outer and inner walls. More than 75 percent of the total diffusion occurs in the prediffuser for all three configurations.

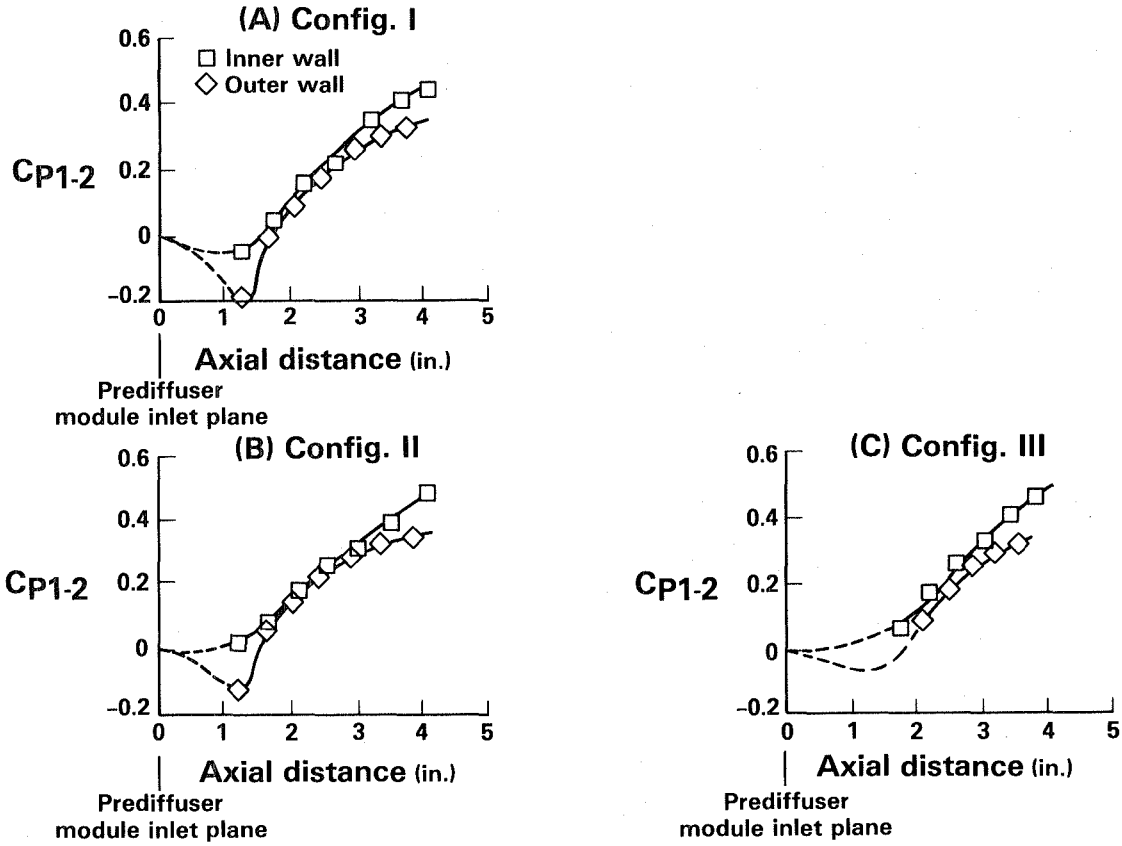

Figure 32 Prediffuser Static Pressure Recovery Distributions with Simulated Combustor (Outer Diameter Peaked Inlet Profiles, Mn = 0.28, Re = 2.5 x 10^5)

TABLE 7
PREDIFFUSER/COMBUSTOR PERFORMANCE
(with baseline struts)

Configuration	C_{p1-2} ID	C_{p1-2} OD	$\tilde{\eta}$	M_{n2}	C_{p1-3} ID	C_{p1-3} OD	λ_{1-2}	λ_{1-3} ID	λ_{1-3} OD
I	0.45	0.34	0.71	0.176	0.58	0.43	0.008	0.022	0.026
II	0.52	0.36	0.74	0.168	0.61	0.48	0.008	0.022	0.026
III	0.47	0.33	0.72	0.176	0.56	0.39	0.008	0.022	0.027
GOAL							$\leq$	0.030	0.030

4.3.2 Total Pressure Losses

The mass averaged total pressure loss λ_{1-3} was nearly identical for all three configurations despite changes in pressure recovery and exit Mach number (see Table 7). Comparison of the prediffuser geometries (see Table 1) indicates that the flow turning angle, β, was 10 degrees for configuration II and 14 degrees for configurations I and III. Less turning in the prediffuser results in a larger incidence angle of the flow on the combustor hood with configuration II. Thus, the lower exit Mach number with configuration II is apparently negated by increased losses associated with flow negotiating the combustor front end at a higher incidence angle. The overall total pressure

loss also includes losses associated with the flow around diffuser case baseline struts and fuel injector supports. Approximately 65-75 percent of the system total pressure losses occur downstream of the prediffuser exit.

Combustor section total pressure losses with the baseline prediffuser/strut combination, as well as with the revised strut design, meet the program goal values (see Table 8). The outer shroud losses reflect those associated with flow over the carburetor tube. The thickened trailing edge on the revised strut increased the dump losses by approximately 0.2 percent P_{T1}.

TABLE 8

COMBUSTOR SECTION PRESSURE LOSSES (% P_{T1})

	Demonstrated		Program Goals
	Baseline Strut	Revised Strut	
Section	5.2	5.5*	5.2-5.3 (cold)
Inner Shroud	2.2	2.40	3.0
Outer Shroud	2.7	2.95	3.0

* Combustor hole pattern was designed with pressure distributions resulting from the baseline strut tests which allowed for higher liner pressure drops. The combustor hole pattern was not changed from the tests incorporating the revised strut design. It is anticipated that program goals would have been met if the proper hole pattern were used.

4.3.3 Branch Flow Splits

The three-branch combustor flow distribution was maintained within the following ranges: inner shroud, 19.7-21.8 percent W_{a2}; combustor hood flow, 17.6-18.7 percent W_{a2}; and outer shroud, 57.5-58.6 percent W_{a2}. Turbine cooling air bleed was fixed at 3.5 percent W_{a1}. The total of the measured branch flows was within 6 percent of the measured rig inlet flow. All mass flow percentages have been corrected to account for measurement inaccuracies in each branch. A mass-weighted correction method was employed to satisfy flow continuity (see Equation 9).

Equation 9

$$W_{a\ \text{branch}}\ _{\text{corrected}} = \left[\frac{W_{a\ \text{branch}}}{\sum W_{a\ \text{branch}}} \right] W_{a\ \text{inlet}}$$

$W_{a\ \text{inlet}}$ is the measured rig inlet airflow rate; $W_{a\ \text{branch}}$ is the measured flow through any branch; and $\sum W_{a\ \text{branch}}$ is sum of all measured branch flows. This method was used for both the simulated combustor and the full combustor flow distribution calculations.

4.4 Phase IV - Sensitivity Study

Initial tests were conducted to ensure that the simulated combustor behaved aerodynamically the same as the full combustor module. Configuration I was tested with each module. Prediffuser wall static pressure distribution and exit total profiles were nominally the same for both modules.

The comparison of flow distribution and total pressure losses between the two modules is shown in Table 9. The results of these tests indicate that there is excellent agreement between the losses for the inner annulus. A slightly higher pressure loss occurred in the outer annulus of the full combustor module. This is attributed to losses associated with flow over the carburetor tubes not included in the simulated combustor module. The higher hood loss with the full combustor module resulted from differences in the volume under the hood. The simulated combustor provided a plenum downstream of the hood inlet, thus allowing the streamlines to readjust before passing through the flow metering bulkhead. In the full combustor module, there is very little volume for the readjustment to take place. Tests were conducted in which hood capture area was decreased to confirm that flow spillage was not the cause of the discrepancy in hood loss levels.

TABLE 9

PERFORMANCE WITH SIMULATED AND FULL COMBUSTOR MODULES
(Baseline Struts)

	Pressure Loss			Flow Split ($\%W_{A2}$)		
	ID	Hood	OD	ID	Hood	OD
Simulated Combustor	0.022	0.018	0.026	20.7	18.7	60.6
Full Combustor	0.022	0.022	0.027	22.4	18.2	59.4

4.4.1 Branch Flow Splits

The sensitivity of the system performance to combustor flow splits is shown in Figure 33. The flow shifts investigated represent perturbations from the baseline level up to 6 percent W_{a2}. The hood flow during the annulus flow shifts remained relatively constant. The increase in the pressure coefficient on the outer wall when flow is shifted from the outer to the inner annulus, is attributed to the reduced acceleration of the flow to achieve the less biased flow split. Correspondingly, the mass averaged total pressure loss decreased with airflow shifts to the inner annulus, as shown in Figure 33.

The rate of change of the pressure coefficient with branch flow splits is an important parameter in establishing stability of the overall system. The stability parameter presented in Figure 34 indicates that the prediffuser/combustor system behaved in a stable (i.e., full flowing) manner throughout the branch flow split range of interest.

4.4.2 Dump Gap

Prediffuser pressure rise and the total pressure loss changes as dump region geometry was varied are presented in Figure 35. The effect of increased dump gap on the prediffuser pressure coefficient is small because of the relatively large baseline non-dimensional dump gap ($X/\Delta R = 2.85$). Increases (up to 0.4 percent P_{T1}) in mass-averaged total pressure loss were measured with the maximum non-dimensional dump gap of 3.45. This represents a 16-percent increase in total pressure loss relative to the baseline configuration. Radial movement of the hood by 6 percent ΔR inboard and 24 percent ΔR outboard (relative to the baseline position) had negligible performance impacts.

4.4.3 Inlet Profile

The effects of variation of inlet total pressure profile on prediffuser and system performance are shown in Table 10. Approximately 2 percent W_{a2} is shifted from the outer shroud to the inner shroud as the peak of the inlet profile is moved to the inner diameter.

TABLE 10

EFFECT OF PREDIFFUSER INLET PROFILE ON PERFORMANCE
(Baseline Strut Configuration)

	C_{p1-2}		$\Delta P_T/P_{T1}$(%)		Flow Splits (%W_{a2})	
Inlet Profile	ID	OD	ID	OD	ID	OD
OD-peaked	0.45	0.34	2.2	2.6	20.7	60.6
Center-peaked	0.46	0.35	2.3	2.8	21.2	59.6
ID-peaked	0.47	0.35	2.3	2.7	22.8	58.5

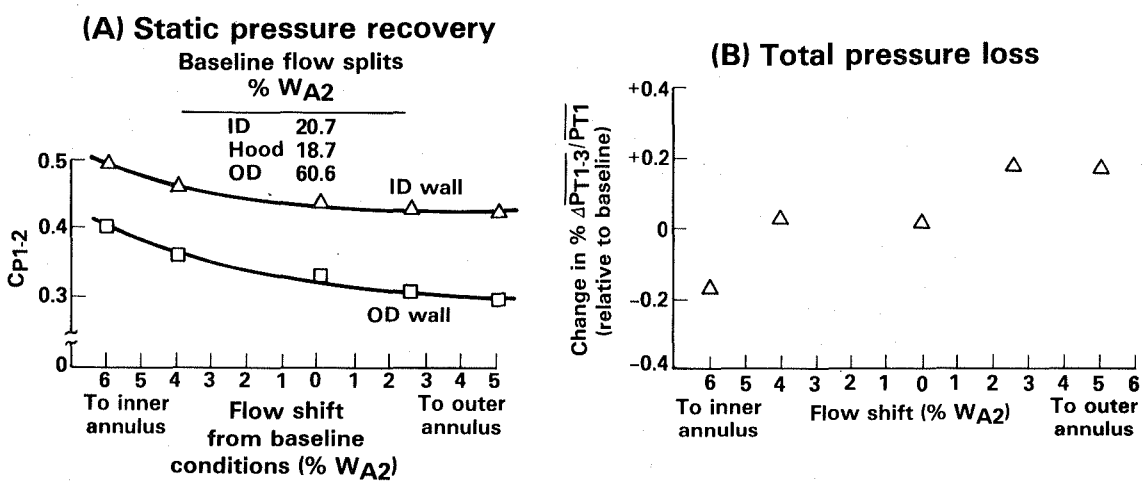

Figure 33 Effect of Combustor Flow Splits on System Performance (Inlet Conditions; Prediffuser Configuration I, Mn = 0.28, Re = 2.5 x 10^5)

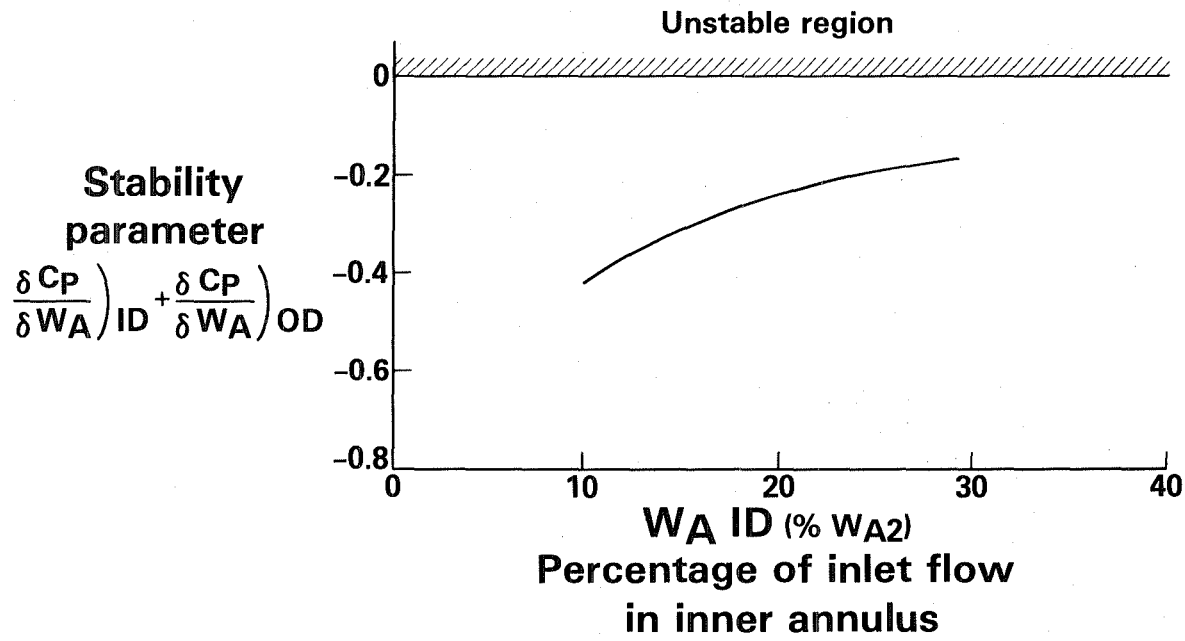

Figure 34 Prediffuser Stability Characteristics as a Function of Downstream Airflow Splits (Based on data from Figure 33)

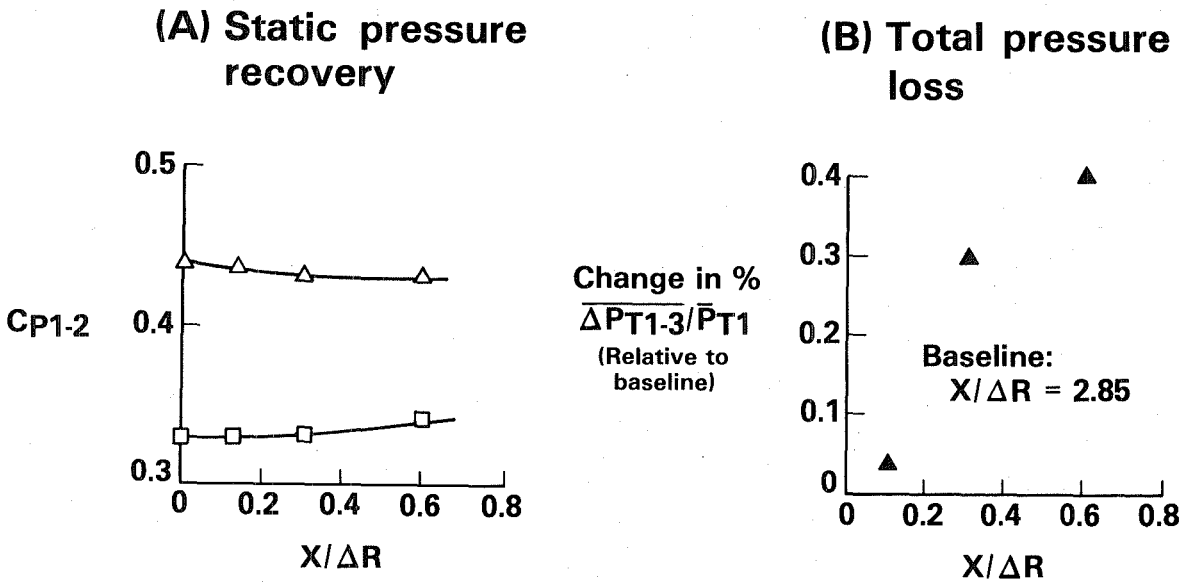

Figure 35 Effect of Dump Gap Spacing on Performance

4.4.4 Air Extraction

The turbine cooling air bleed at the prediffuser inlet and extraction through the outer wall in the dump region (customer bleed) did not significantly affect performance. Customer bleed flow of 9.3 percent W_{a2} was regarded as an average installation requirement for the engine. For the customer bleed case, the major change in flow occurred in the outer annulus. The relative flow distribution in the three branches downstream of the dump plane (customer) bleed is similar both with and without bleed extraction, indicating a minimum impact on the pilot zone combustion process. The effects of these bleed air extractions on system performance are tabulated in Table 11.

TABLE 11

EFFECT OF BLEED AIR EXTRACTION ON PERFORMANCE

(a) Turbine Cooling Air Bleed (Configuration I)

	C_p 1-2	
	ID	OD
No Bleed	0.37	0.35
3.5% W_{a1}	0.37	0.36

(b) Customer Bleed (Configuration II)

	C_{p1-2}		P_T/P_{T1} Baseline Struts		Flow Splits (%W_{a2})		
	ID	OD	ID (%)	OD	ID	Hood	OD
No Bleed	0.52	0.36	2.2	2.6	20.7	18.7	60.6
9.3% W_{a2}	0.52	0.36	2.2	2.6	18.7	17.1	54.9

4.4.5 System Flow Uniformity

A complete pressure map of the diffuser/combustor section is presented in Figures 36 through 42. The results are from tests conducted with the baseline configuration and a full combustor module.

Figure 36 shows that the inlet pressure field is circumferentially uniform at any span location to within 0.3 percent of the average inlet total pressure.

The prediffuser outer wall static pressure distributions are presented in Figure 37. The first row of measurements reflect local disturbances caused by the slight mismatching of the instrumentation section to the prediffuser section. The flow readjusts itself by the second axial station (approximately one X/ R) and is uniform at the exit plane. The local elevation of static pressure at the 180-degree position results from the instrumentation being in line with a downstream diffuser case strut. The pressure field indicates a local back-pressuring caused by this strut.

The prediffuser exit total pressure profiles, as measured with diffuser case strut leading edge instrumentation, are shown in Figure 38. The total and static pressure field in the inner and outer shroud annuli are presented in Figures 39 through 42. A high degree of uniformity exists at the carburetor tube feed plane in the outer annulus. Radial static pressure gradients (case wall to liner wall) in both annuli are insignificant. Most of the static pressure recovery occurred in the prediffuser, with approximately 25 percent in the shroud annuli.

4.5 Phase V - Revised Strut Evaluation

The objective of this phase of testing was to assess the performance of a thickened trailing edge strut design. Rig inlet Mach number was varied over a wide range and total pressure losses to the inner and outer shroud were measured. The results of the dump loss measurements are presented in Figure 43 and in Table 8. The thickening of the trailing edge from 0.120 inch to 0.300 inch as well as the increased taper near the inner and outer diameter case walls (for ease of casting) result in an increase in the dump losses of approximately 0.2 percent P_{T1}.

Wake rake traverses were conducted behind both the baseline and revised struts at the inlet to the inner shroud annulus (approximately 2.5 in. downstream of the strut trailing edge). The width of the eleven element wake rake encompassed 62 percent of the nominal distance between the struts. Circumferential movement of the rake by one full width therefore ensured more than 100 percent circumferential coverage of the distance between struts. The total pressure characteristics downstream of the struts are presented in Figure 44 at various inner shroud span locations. No wake characteristics are evident in either strut data. The location of the strut trailing edge in the dump region near the combustor hood, where the flow is rapidly accelerating to the shrouds, provides good mixing and apparently dissipates any generated wake before the deceleration is initiated in the shrouds.

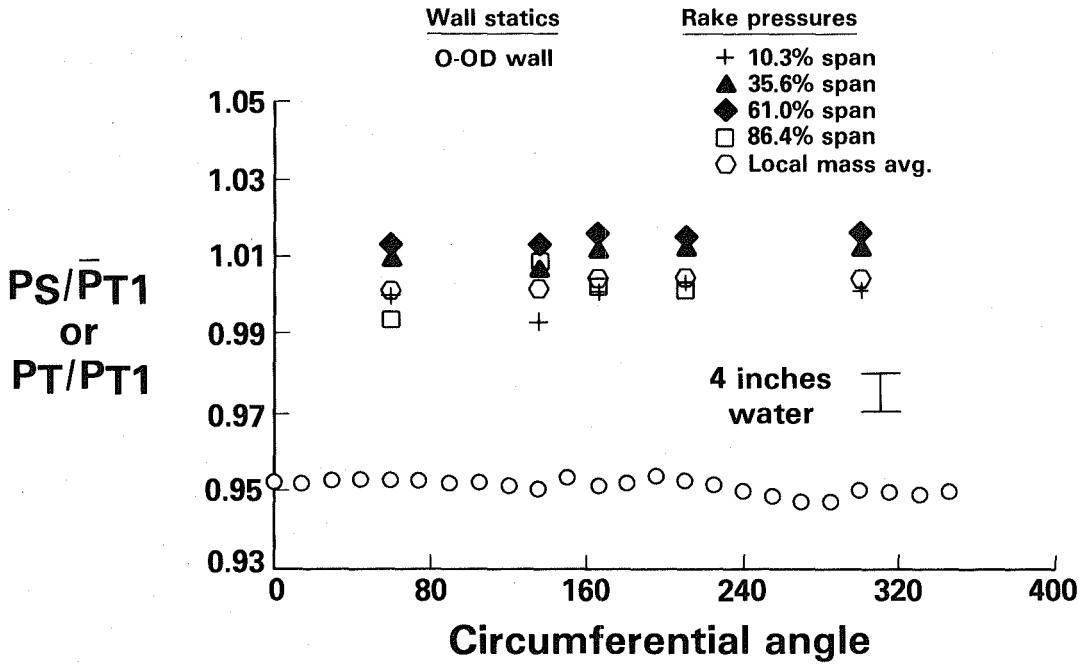

Figure 36 Prediffuser Inlet Pressure Map

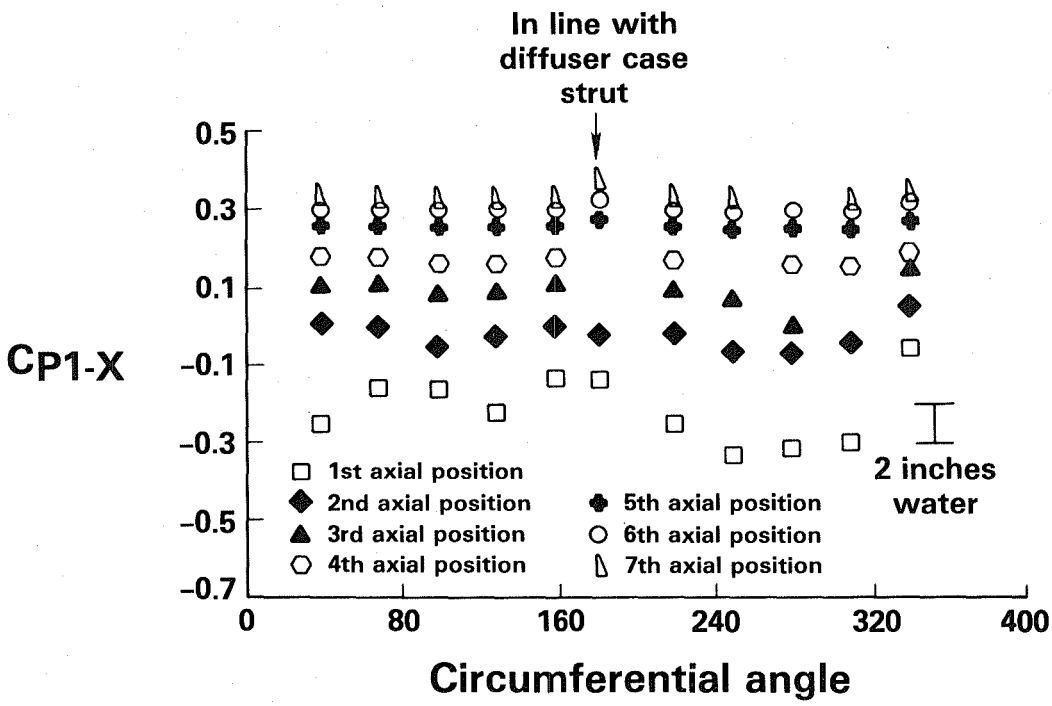

Figure 37 Static Pressure Recovery on Outer Prediffuser Wall

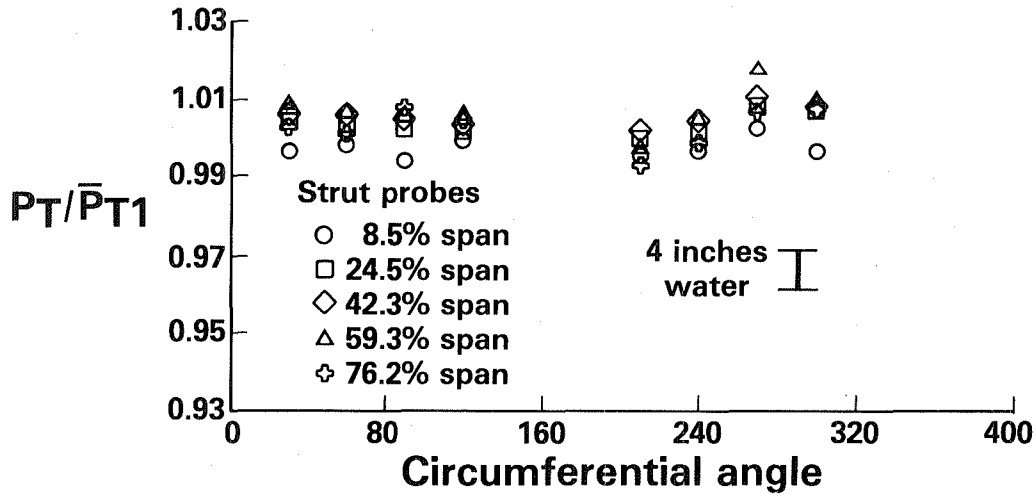

Figure 38 Prediffuser Exit Total Pressure Map

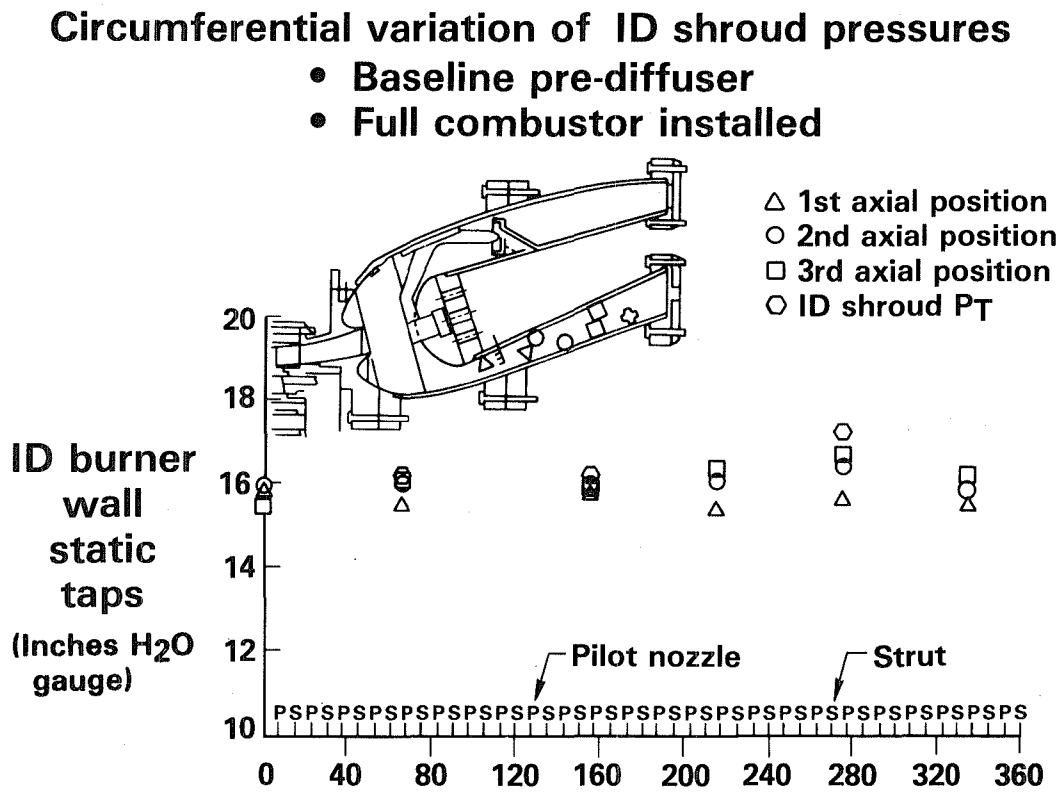

Figure 39 Inner Annulus Pressure Map (Liner)

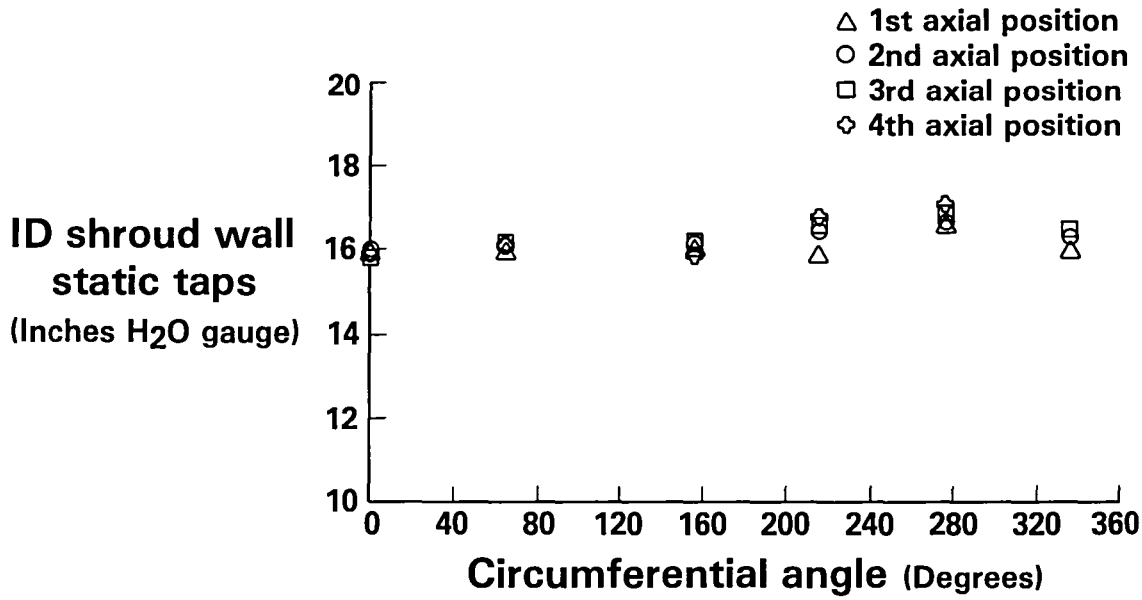

Figure 40 Inner Annulus Pressure Map (Diffuser Case)

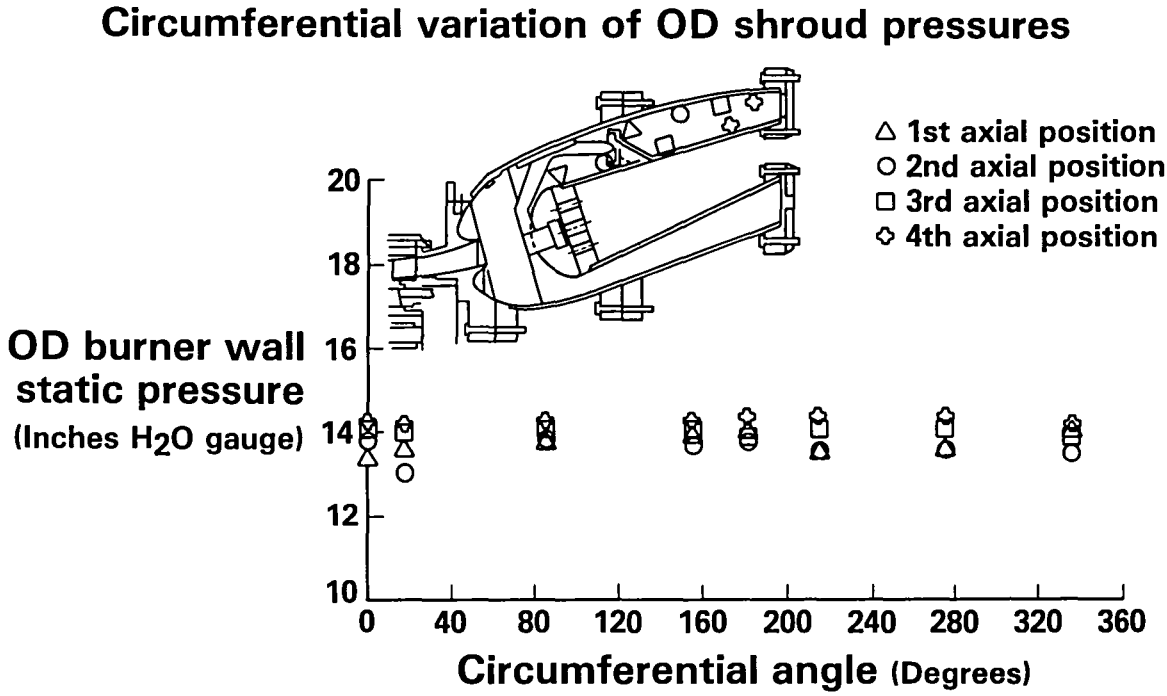

Figure 41 Outer Annulus Pressure Map (Liner)

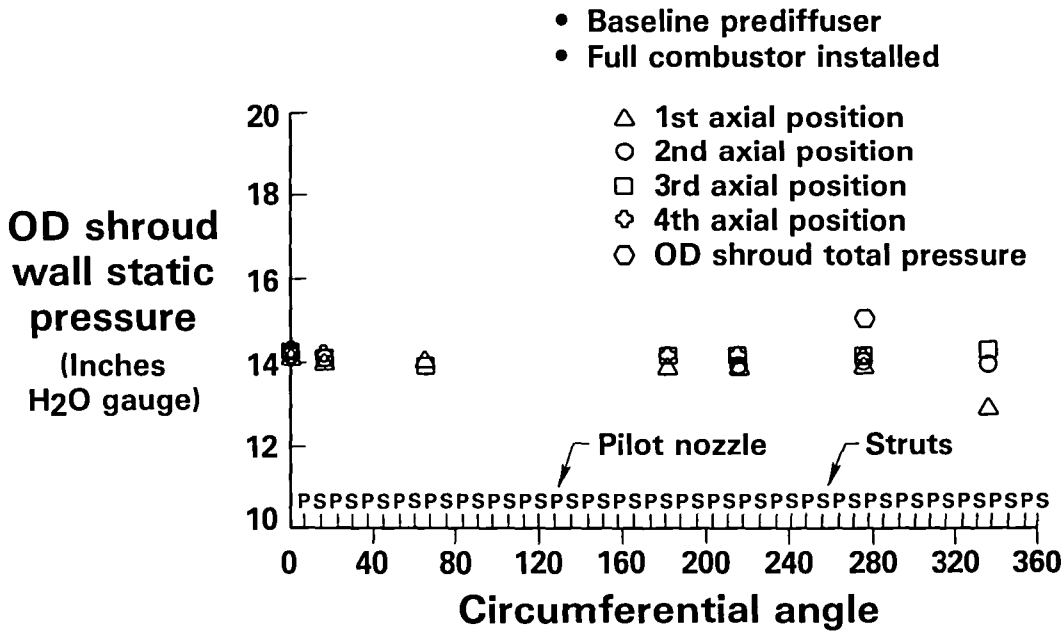

Figure 42 Outer Annulus Pressure Map (Diffuser Case)

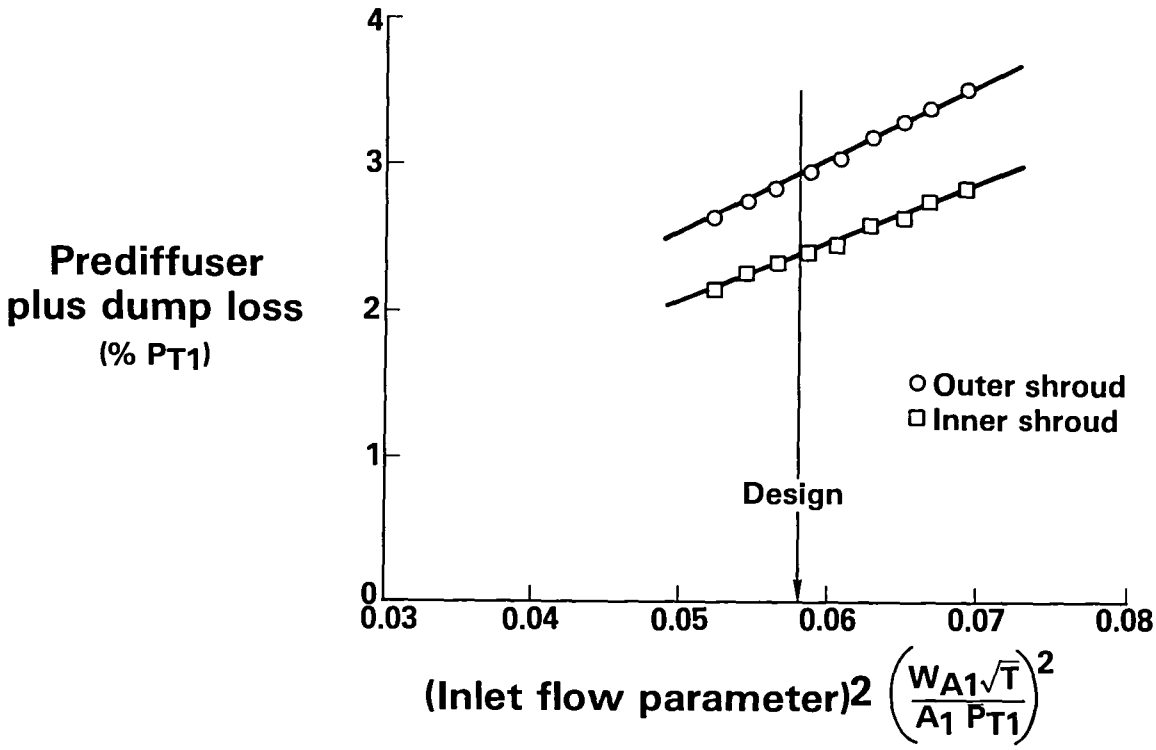

Figure 43 Dump Loss Characteristics with the Revised Strut Design

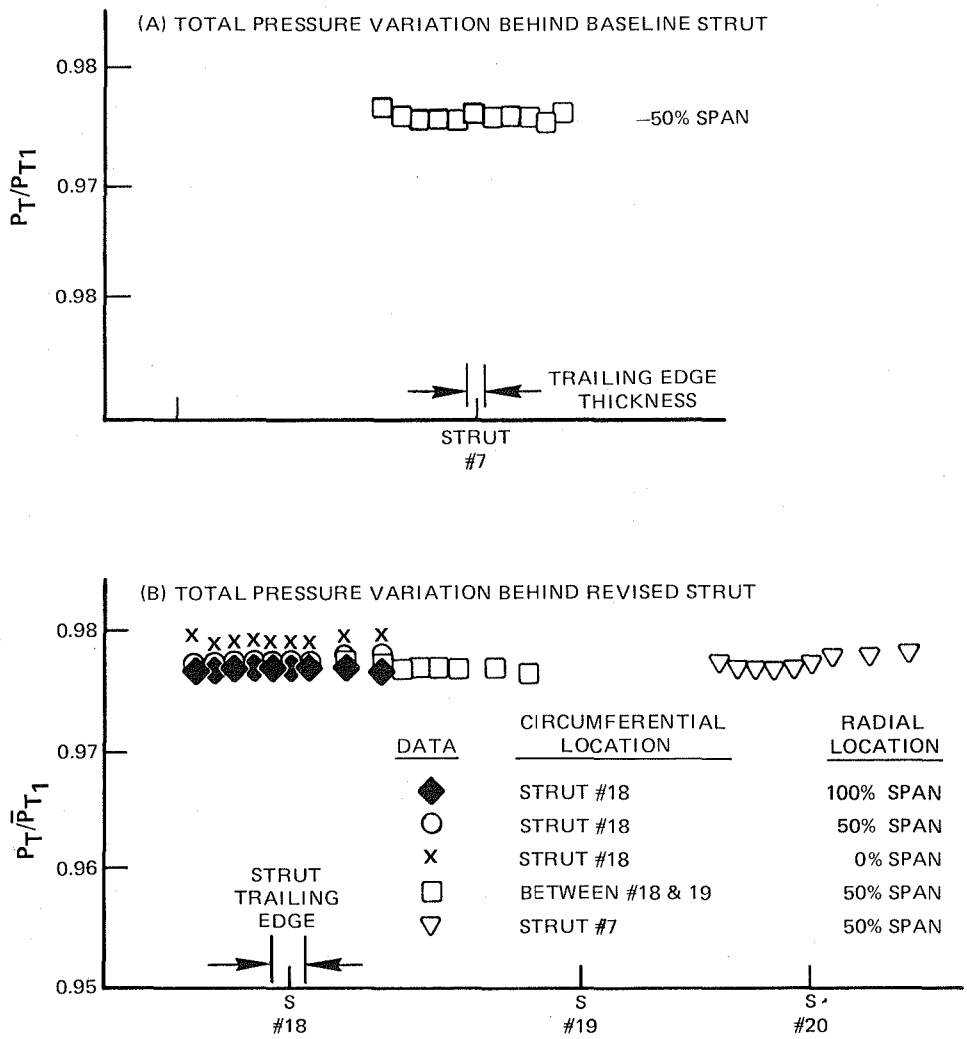

Figure 44 Inner Shroud Wake Rake Traverse Results

5.0 Conclusions

Tests conducted to evaluate the aerodynamic performance of several prediffuser/combustor systems have shown that:

1. All three prediffuser configurations operated without flow separation over a wide range of inlet flow conditions.

2. Configuration III (short $L/\Delta R$) was judged to be closer to separation than the other two configurations.

3. All three prediffuser/combustor systems met the program pressure loss goals.

4. Although changes in prediffuser performance due to differences in geometry were evident, overall system losses were nearly the same for the three systems that were tested. Specifically, the prediffuser performance improvement achieved with the larger area ratio configuration was apparently negated by the higher flow incidence angle on the combustor hood.

5. For the range of variables investigated, the most significant design parameter influencing system performance is the dump gap. Changes in flow split, radial combustor location, inlet profile, and bleed air extraction had minimal impact.

6. Almost all the pressure rise of a given system occurs in the prediffuser, but nearly all the loss occurs in the dump, hood, and annuli surrounding the combustor. Care must be exercised in the aerodynamic integration of the combustor front-end with the prediffuser to minimize pressure losses.

7. Significant spanwise variations in static pressure occur in the curved wall prediffuser with combustor backpressuring and the flow splits of the present study. This pressure distribution could cause pronounced secondary flows on surfaces, such as struts, located in the prediffusers.

8. Based on conclusions 2 and 4, Configuration I (Baseline) was incorporated into the combustor component and sector rig programs.

9. Wake rake traverse data indicated no wakes or pressure maldistributions in the inner shroud.

REFERENCES

1. Follansbee, P.S., Dils, R.R., "Experimental Clean Combustor Program-Turbulence Characteristics of Compressor Discharge Flows," NASA CR-135277, October 1977.

2. Stevens, S.J., Nayak, U.S.L., Preston, J.F., Robinson, P.J. Scrivener, C.T.J., "The Influence of Compressor Exit Conditions on the Performance of Combustor-Dump Diffusers," AIAA Paper 76-726, July 1976.

3. Adenubi, S.O., "Performance and Flow Regime of Annular Diffusers with Axial Turbomachine Discharge Inlet Conditions," ASME Paper 75-WA/FE-5, December 1975.

DISTRIBUTION LIST

Title: Energy Efficient Engine - Component Development and Integration
Diffuser/Combustor Model Technology Report

Contract: NAS3-20646

(One copy per addressee unless otherwise noted in parenthesis)

GOVERNMENT AGENCIES

NASA Headquarters
600 Independence Ave., SW
Washington, D.C. 20546
Attention: RTP-6/R. S. Colladay
RTM-6/L. Harris
RJP-2/D. J. Poferl (2 copies)
Library

NASA-Lewis Research Center
21000 Brookpark Road
Cleveland, OH 44135

Attention:	D. L. Nored	MS 301-2
	C. C. Ciepluch	MS 301-4
	J. W. Schaefer	MS 301-4
	L. E. Macioce	MS 301-4
	J. A. Ziemianski	MS 49-6
	Library	MS 60-3 (2 copies)
	Report Control Office	MS 5-5
	Technology Utilization Office	MS 3-19
	W. L. Stewart	MS 3-5
	M. A. Beheim	MS 86-1
	J. R. Esterly	MS 500-207
	M. J. Hartmann	MS 5-3
	R. A. Rudey	MS 86-5
	R. J. Weber	MS 500-127
	W. C. Strack	MS 500-127
	R. E. Jones	MS 86-6
	D. C. Mikkelson	MS 86-7
	R. M. Purgert	MS 500-303
	J. A. Biaglow	MS 86-6
	D. B. Ercegovic	MS 86-6
	R. W. Niedzwiecki	MS 86-6
	J. S. Fear	MS 86-6
	A. J. Powers	MS 500-127
	R. G. Willoh, Jr.	MS 500-207
	D. A. Petrash	MS 86-6
	AFSC Liaison Office	MS 501-3
	Army R&T Propulsion Lab	MS 106-2

NASA Ames Research Center
Moffett Field, CA 94035
Attention: 202-7/M.H. Waters
202-7/L.J. Williams
Library

NASA Langley Research Center
Langley Field, VA 23365
Attention: R. Leonard
D. Maiden
Library

NASA Dryden Flight Research Center
P.O. Box 273
Edwards, CA 93523
Attention: J.A. Albers
Library

NASA Scientific and Technical Information Facility
P.O. Box 33
College Park, MD 20740
Attention: Acquisition Branch (10 copies)

Department of Defense
Washington, D.C. 20301
Attention: R. Standahar 3D1089 Pentagon

Wright-Patterson Air Force Base
Dayton, OH 45433
Attention:

H.J.P. VonOhain	AFAPL/CCN
E.C. Simpson	AFAPL/TB
H.I. Bush	AFAPL/TB
E.E. Bailey (NASA Liaison)	AFAPL/DO
P.P. Carmichael	ASD/XFHI
F. Ellis	ASD/YZN
Col. C.E. Painter	ASD/EN

Eustis Directorate
U.S. Army Air Mobility
R&D Laboratory
Fort Eustis, VA 23604
Attention: J. Lane, SAVDL-EU-Tapp

Department of Transportation
NASA/DOT Joint Office of
Noise Abatement
Washington, D.C. 20590
Attention: C. Foster

NAVY Department
Naval Air Systems Command
Washington, D.C. 20361
Attention: W. Koven AIR-03E
J.L. Byers AIR-53602
E.A. Lichtman AIR-330E
G. Derderian AIR-5362C

NAVAL Air Propulsion Test Center
Trenton, NJ 08628
Attention: J.J. Curry
A.A. Martino

U.S. Naval Air Test Center
Code SY-53
Patuxent River, MD 20670
Attention: E.A. Lynch

USAVRAD Command
PO BOX 209
St. Louis, MO 63166
Attention: Robert M. Titus (ASTIO)

Federal Aviation Administration
Noise Abatement Division
Washington, D.C. 20590
Attention: J. Woodhall

Environmental Protection
Agency
1835 K Street, NW
Washington, D.C. 20460
Attention: J. Schettino
J. Tyler

Environmental Protection
Agency
2565 Plymouth Road
Ann Arbor, MI 48105
Attention: R. Munt

Federal Aviation Administration
12 New England Executive Park
Burlington, MA 18083
Attention: Jack A. Sain, ANE-200

ENGINE MANUFACTURERS

Curtiss Wright Corporation
Woodridge, NJ 07075
Attention: S. Lombardo
S. Moskowitz

Detroit Diesel Allison Div. G.M.C
P.O. Box 894
Indianapolis, IN 46206
Attention: W.L. McIntire

Detroit Diesel Allison Div. G.M.C.
333 West First St.
Dayton, OH 45402
Attention: F.H. Walters

The Garrett Corporation
AIResearch Manufacturing Co.
Torrance, CA 90509
Attention: F.E. Faulkner

Cummins Engine Co.
Technical Center
500 S. Poplar
Columbus, IN 47201
Attention: J.R. Drake

AVCO/Lycoming
550 S. Main Street
Stratford, CN 06497
Attention: H. Moellmann

AIResearch Manufacturing Co.
111 South 34th Street
P.O. Box 5217
Phoenix, AZ 85010
Attention: C.E. Corrigan
(93-120/503-4F)

Williams Research Co.
2280 W. Maple Road
Walled Lake, MI 48088
Attention: R. VanNimwegen
R. Horn

The Garrett Corporation
AIResearch Manufacturing Co.
402 S. 36 Street
Phoenix, AZ 85034
Attention: F.B. Wallace

Teledyne CAE, Turbine Engines
1330 Laskey Road
Toledo, OH 43612
Attention: W.Q. Wagner

General Electric Co./AEG
One Jimson Road
Evendale, OH 45215
Attention: T. Hampton (3 copies)
T.F. Donohue
B.L. Koff

General Electric Co./AEG
1000 Western Ave.
Lynn, MA 01910
Attention: R.E. Neitzel

Pratt & Whitney Aircraft
Group/UTC
Government Products Division
P.O. Box 2691
West Palm Beach, FL 33402
Attention: B. A. Jones

Pratt & Whitney Aircraft
Group/UTC
Commercial Products Division
East Hartford, CT 06108
Attn: W. Gardner (3 copies)
W.H. Sens

The Garrett Corporation
AIResearch Aviation Company
19201 Susana Road
Compton, CA 90221
Attention: N. J. Palmer

AIRFRAME MANUFACTURERS

Boeing Commercial Airplane Co.
P.O. Box 3707
Seattle, WA 98124
Attention: P.E. Johnson MS 9H-46*
D.C. Nordstrom MS 73-01*

Boeing Aerospace Co.
P.O. Box 3999
Seattle, WA 98124
Attention:
D.S. Miller MS 40-26
H. Higgins

The Boeing Co., Wichita Division
Wichita, KS 67210
Attention: D. Tarkelson

Gates Learjet Corp.
P.O. Box 7707
Wichita, KS 67277
Attention: E. Schiller

Douglas Aircraft Co.
McDonnell Douglas Corp
3855 Lakewood Boulevard
Long Beach, CA 90846
Attention: R.T. Kawai Code 36-41
M. Klotzsche

McDonnell Aircraft Co.
McDonnell Douglas Corp
P.O. Box 516
St. Louis, MO 63166
Attention: F.C. Claser
Dept. 243

Lockheed California Co.
Burbank, CA 91502
Attention: J.F. Stroud, Dept. 75-42
R. Tullis, Dept. 75-21
J. I. Benson

Lockheed Georgia Co.
Marietta, GA 30060
Attention: H.S. Sweet

General Dynamics Convair
P.O. Box 80847
San Diego, CA 92138
Attention: S. Campbell, MZ 632-00

Grumman Aerospace Corp.
South Oyster Bay Road
Bethpage, NY 11714
Attention: C. Hoeltzer

Rockwell International
International Airport
Los Angelos Division
Los Angelos, CA 90009
Attention: A.W. Martin

AIRLINES

American Airlines
Maint. & Engr. Center
Tulsa, OK 74151
Attention: W.R. Neeley

Delta Airlines, Inc.
Hartsfield-Atlanta
International Airport
Atlanta, GA 30320
Attention: C.C. Davis

Eastern Airlines
International Airport
Miami, FL 33148
Attention: A.E. Fishbein

TransWorld Airlines
605 Third Avenue
New York, NY 10016
Attention: A.E. Carrol

Pan American World Airways, Inc.
JFK International Airport
Jamica, NY 11430
Attention: L. H. Allen, Jr.
A. MacLarty

United Airlines
San Francisco
International Airport
Maint. Operations Cntr.
San Francisco, CA 94128
Attention: J.J. Overton

OTHERS

Hamilton Standard
Bradley Field
Windsor Locks, CT 06096
Attention: P.J. Dumais, MS 1A-3-1
A.T. Reiff, MS 1-2-2

Westinghouse Electric Corp.
P.O. Box 5837
Beulah Road
Pittsburgh, PA 15236
Attention: Library

FluiDyne Engineering Corp.
5900 Olson Memorial Highway
Minneapolis, MN 55422
Attention: J.S. Holdhusen

Univ. of Tennessee
Space Institute
Tullahoma, TN 37388
Attention: Dr. V. Smith

Rohr Corporation
P.O. Box 878
Foot & H Street
Chula Vista, CA 92012
Attention: Library

TRW Equipment Group
TRW Inc.
23555 Euclid Ave.
Cleveland, OH 44117
Attention: I. Toth

Solar Division
International Harvester
2200 Pacific Highway
San Diego, CA 92112
Attention: Library

Aerospace Corporation
R & D Center
Los Angelos, CA 90045
Attention Library

Gas Dynamics Laboratories
Aerospace Engineering Building
University of Michigan
Ann Arbor, MI 48109
Attention: Dr. C.W. Kaufmann

George Shevlin
P.O. Box 1925
Washington, D.C. 20013

Massachusetts Inst. of Technology
Dept. of Astronautics & Aeronautics
Cambridge, MA 02139
Attention: Jack Kerrebrock

Brunswick Corporation
2000 Brunswick Lane
Deland, FL 32720
Attention: A. Erickson

Massachusetts Inst. of Technology
Dept. of Structural Mechanics
Cambridge, MA 02139
Attention: James Mar

Purdue University
School of Mechanical Engineering
West Lafayette, Indiana 47907
Attention: Prof. A. H. Lefebre
Prof. A. M. Mellor
Prof. M. R. L'Ecuyer

End of Document